Proteins Containing Oxo-Bridged Dinuclear Iron Centers: A Bioinorganic Perspective

JOHN B. VINCENT, GAY L. OLIVIER-LILLEY, and BRUCE A. AVERILL*

Department of Chemistry, University of Virginia, Charlottesville, Virginia 22901

Received May 8, 1990 (Revised Manuscript Received September 17, 1990)

Contents

I. Introduction

In recent years, evidence has accumulated that proteins containing oxo-bridged dinuclear iron centers are widespread in biology. The crystal structure of hemerythrin, an O_2-transport protein from marine worms and the prototypical member of this group of proteins, was reported in 1981 and revealed the presence of two bridging carboxylate ligands in addition to an oxo bridge. Subsequent spectroscopic experiments strongly implicated the presence of a similar unit in ribonucleotide reductase, which has been confirmed very recently by a crystal structure of the enzyme (albeit with only a single bridging carboxylate). Synthetic work over the past 10 years has demonstrated that the bis(μ-carboxylato)(μ-oxo) and mono(μ-carboxylato)(μ-oxo)diiron cores assemble spontaneously in aqueous solution under a variety of conditions and with a variety of terminal ligands. Given the intrinsic stability of the (μ-oxo)diiron unit and its propensity to "self-assembly" reactions, it is perhaps not surprising that additional examples in biology have been identified by comparison of corresponding spectroscopic and physical properties. Examples of these include the purple acid phosphatases, a group of hydrolytic enzymes found in mammals, plants, and microbes, and methane monooxygenase, which is responsible for the initial step in methane uptake by methanotrophic bacteria. Members of this class exhibit certain common spectroscopic signatures: EPR signals at $\leq$30K with g_{av} = 1.7–1.8 in the mixed-valence Fe(II)–Fe(III) form and antiferromagnetic coupling between the ferric ions in the oxidized form.

The available structural and spectroscopic data indicate a high degree of congruence in the dinuclear iron sites of these proteins, yet they exhibit an amazing variety of biological functions: O_2 transport, O_2 activation and insertion into an unactivated C–H bond, phosphate ester hydrolysis, and electron transfer. In fact, it can be argued that the Fe_2O unit constitutes the most versatile iron center yet encountered in biology. The more familiar heme centers are capable of both electron transfer and O_2 binding and activation, but not nonredox chemistry, while iron–sulfur clusters are known to participate in electron-transfer and nonredox chemistry, but not directly in O_2 chemistry. It now appears as if proteins containing the Fe_2O unit are capable of all these functions, and it seems likely that new examples remain to be discovered.

Consequently, a review of the properties of dinuclear oxo-bridged iron proteins seems timely. The present article focuses on the spectroscopic and physical properties of the dinuclear iron centers. Its major theme is the exploration of how the intrinsic properties of a dinuclear oxo-bridged iron center are modulated by a particular polypeptide environment (insofar as this can be determined from the available data) and utilized in a given biological function. This review is intended to be comprehensive with regard to published work addressing the above points, but coverage of the more biochemical and physiological aspects of these proteins is necessarily selective.

This class of proteins has attracted a great deal of interest in recent years, as evidenced by the relatively large number of original publications cited and by the availability of numerous review articles addressing some of the topics covered here. Thus, reviews devoted specifically to hemerythrin,[1,2] purple acid phosphatases,[3,4] and ribonucleotide reductase[5] are available, as are shorter reviews of broader scope focusing more heavily on synthetic model chemistry.[6,7] The role of oxo-bridged dinuclear iron centers in oxygen chemistry has been summarized,[8] and an overview of the spectroscopic and reactivity properties of these proteins has recently appeared.[9] Because of the very recent publication of an exhaustive review of the structure and properties of synthetic dinuclear iron complexes in this journal,[10] only those synthetic complexes that most closely approximate key features of a particular dinuclear oxo-bridged iron protein have been included in this article.

II. Hemerythrin

Hemerythrin (Hr) is an oxygen-binding protein containing two nonheme iron atoms per subunit.[1,2,11] The protein has been isolated from a variety of marine invertebrates, including sipunculids (peanut worms), annelids (segmented worms), priapulids, and brachiopods (lampshells). While the protein is most often found as an octamer, monomeric (myohemerythrin), dimeric, trimeric, and tetrameric forms are also known. In general, oxygen binding by hemerythins does not exhibit cooperativity (for exceptions see ref 12). Despite the differences in quaternary structure, the subunit molecular weight is always approximately 13500–13900 Da; subunits in a given protein are identical (or very nearly so).

0009-2665/90/0790-1447$09.50/0

John B. Vincent was born in Cape Girardeau, MO in 1962 and graduated with a B.S. degree in chemistry and mathematics from Murray State University in 1984. In 1988, he received his Ph.D. degree in chemistry (majoring in inorganic chemistry) at the University of Indiana under George Christou. He is currently a postdoctoral fellow under Bruce A. Averill at the University of Virginia.

Gay Olivier-Lilley was born and raised in Grand Rapids, MI. She received her B.S. degree in 1980 from Olivet Nazarene College, Kankakee, IL. In 1985, she completed an M.S. degree studying inorganic synthesis under the direction of Professor Bruce Averill at the University of Virginia. After a brief intermission during which she worked in the area of biophysical chemistry at Loyola University of Chicago with Professor Leslie W. M. Fung, she returned to the University of Virginia where she is now completing her Ph.D. in bioinorganic chemistry.

Bruce A. Averill was born in Ohio in 1948 and grew up in New England. He received a B.S. in chemistry from Michigan State University in 1969 followed by a Ph.D. in inorganic chemistry with Dick Holm at M.I.T. in 1973. Subsequently, he spent three years learning biochemistry on NIH and NSF postdoctoral fellowships with Bob Abeles at Brandeis University and Bill Orme-Johnson at the University of Wisconsin, Madison. In 1976, he returned to Michigan State University as assistant professor of chemistry. He was named an Alfred P. Sloan Foundation Fellow and promoted to associate professor in 1981. In 1982, he moved to the Chemistry Department at the University of Virginia, where he is currently a professor of chemistry. His research interests range from the isolation and characterization of novel metalloproteins to the synthesis of Mo–Fe–S clusters as models for the FeMo-cofactor of nitrogenase to the synthesis of new low-dimensional conducting materials and superconductors.

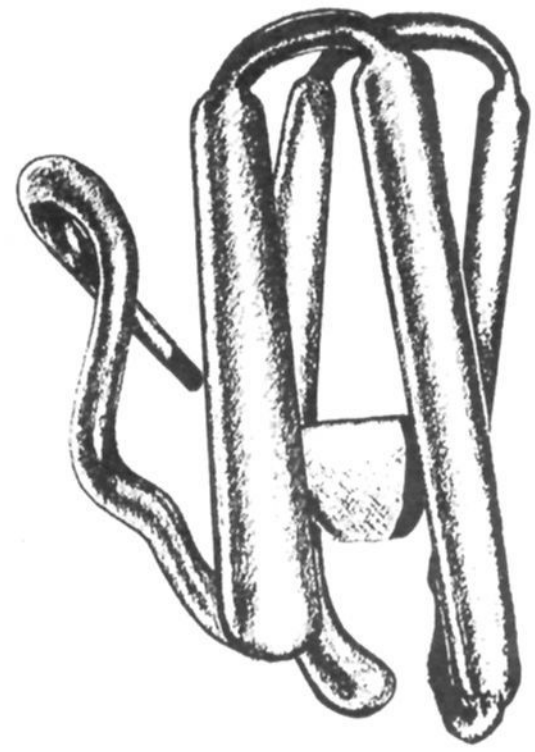

Figure 1. Tertiary structure of hemerythrin showing four antiparallel α-helices and central Fe_2 unit (reprinted from ref 15; copyright 1975 National Academy of Sciences).

In nature, subunits are found in either of two oxidation levels related by $2e^-$/pair of Fe atoms: deoxyHr (the reduced form prior to O_2 binding) and oxyHr (with O_2 bound). DeoxyHr can be oxidized chemically in the absence of dioxygen to produce metHr. This form readily binds a monodentate ligand (L); the corresponding complex is named metLHr (for example, metazidohemerythrin, abbreviated metN_3Hr). One-electron oxidation of deoxyHr or one-electron reduction of metHr produces the semimet level, intermediate between deoxy and met; this form is, however, unstable toward disproportionation. The semimet forms produced by reduction of metHr, $(semimet)_R$, and by oxidation of deoxyHr, $(semimet)_O$, have been found to exhibit distinct spectroscopic properties.[13,14]

The most detailed information on the structure and function of hemerythrin has come from X-ray crystallographic studies.[15–29] Each subunit of Hr is composed of four antiparallel α-helices (Figure 1), which comprise approximately 75% of the amino acid residues (in agreement with predictions of earlier circular dichroism studies).[30,31] The virtually identical tertiary structures of subunits from proteins of varying sources is somewhat surprising, given the fact that there is only approximately 40% sequence homology,[32–35] a situation reminiscent of hemoglobin and myoglobin. Two iron atoms are bound in a dinuclear iron center, which is located roughly in the center of the four α-helices. Thus, the overall structure possesses approximate C_2 symmetry, with the symmetry axis running through the center of and parallel to the four helices. Interestingly, the sequences of Hr have an apparent repeat that suggests that Hr is the result of duplication and fusion of the gene for a mononuclear iron protein.[29] As the resolution of the electron density map about the diiron center improved and the iron-binding ligands became observable, the iron ligation became quite controversial, and groups working on the respiratory protein from different sources developed different models for the iron coordination.[27,28] However, refinement of the structure of the metazido forms to R values of 17.5% (octameric)[22] and 15% (myoHr)[24] have given rise to a consistent picture of the iron ligation (Figure 2). Both irons are

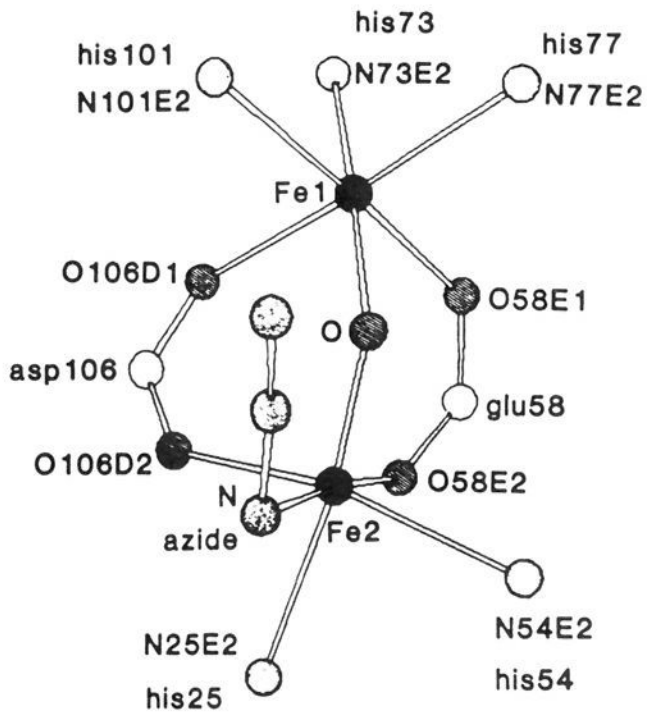

Figure 2. Structure of dinuclear iron center of metazidohemerythrin (reprinted from ref 21; copyright 1983 Munksgaard).

TABLE I. Selected Mean Bond Angles and Distances for Methemerythrin and Metazidohemerythrin (Ref 21)

	met	$metN_3$
Fe···Fe	3.21 Å	3.25 Å
$Fe–O_{oxide}$	1.68, 1.92 Å	1.64, 1.89 Å
$Fe–O_{Asp}$	2.03, 2.10 Å	2.16, 2.20 Å
$Fe–O_{Glu}$	2.04, 2.28 Å	2.33, 2.24 Å
$Fe–N_{His}$	2.15, 2.19 Å (five-coord Fe)	2.22, 2.25 Å
	2.17, 2.24, 2.31 (six-coord Fe)	2.27, 2.29, 2.13 Å
$Fe–N_{azide}$		2.34 Å
$Fe–O_{oxide}–Fe$	127°	135°
$Fe–N1_{azide}–N2_{azide}$		111°

octahedrally coordinated and bridged by an oxide ion (as predicted by previous magnetic susceptibility and electronic studies (vide infra)), with short Fe–O distances (ca. 1.64–1.92 Å). The protein provides two bridging carboxylate groups from the side chains of an aspartate and a glutamate residue and five imidazole ligands from histidines. One iron is coordinated by three histidines, the other by two. Coordination of the second iron is completed by a monodentate azide ligand. A collection of bond distances and angles is given in Table I. Iron ligands are provided by each of the four α-helices. Two helices furnish ligands to one iron, while the other two α-helices provide ligands to the second iron. Additionally, the structure of metHr (previously referred to erroneously as metaquoHr) has been refined to an R factor of 17.3%.[22] The structure of the diiron center differs from that of $metN_3Hr$ mainly in that the azide-binding site is vacant, leaving the second iron only five coordinate. The change in coordination number results in subtle changes in the geometry about both irons (Table I).

X-ray diffraction studies of oxyHr have achieved sufficient resolution to allow the determination of the structure of the dioxygen binding site. It is found that dioxygen binds to a single Fe, the five-coordinate Fe of metHr, in an end-on fashion, similar to azide.[23] The proximity of the bound O_2 to the oxide bridge, the only hydrogen-bond acceptor near the site, suggested the presence of a hydrogen bond between the bridging oxo ligand and the oxygen of O_2 not bound to the metal; this and the binding mode of the peroxide have been borne

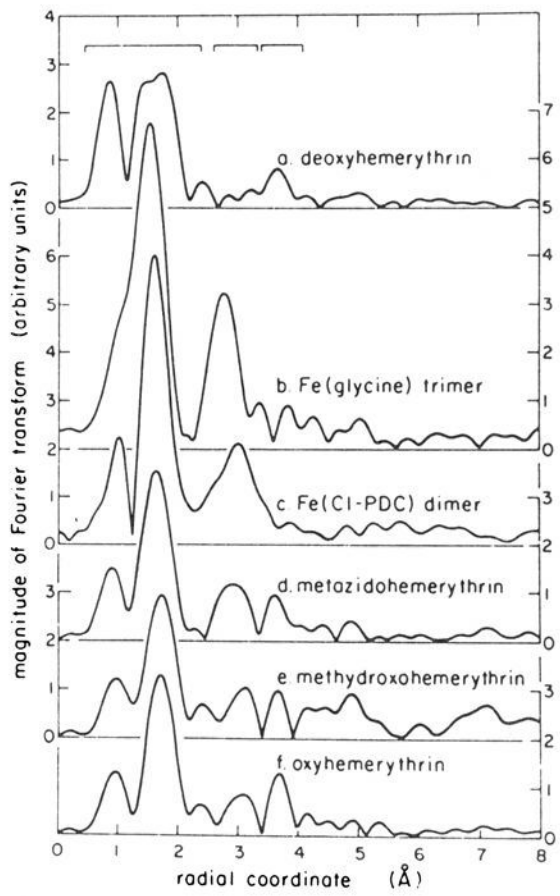

Figure 3. Fourier transform of Fe K-edge EXAFS data for various forms of hemerythrin and model compounds (reprinted from ref 36; copyright 1982 American Chemical Society). Fe(glycine) trimer = $[Fe_3O(glycinato)_6(H_2O)_3](ClO_4)_7$; Fe(Cl(PDC)) dimer = $[Fe_2O(4\text{-chloro-2,6-pyridinedicarboxylato})_2(H_2O)_4]\cdot 4H_2O$.

out by resonance Raman studies (vide infra). Difference electron-density maps between deoxyHr and metHr indicate that the deoxyHr metal complex appears to retain the same ligands and symmetry as the met form, although the results are not conclusive as the deoxy electron map is at low resolution.[23] One significant difference between the iron centers of the two forms appears to be a lengthening of the metal···metal separation in going from metHr to deoxyHr.

X-ray diffraction studies on Hr have been complemented nicely by X-ray absorption studies.[25,36-40] Fourier transforms (FT's) of the EXAFS data for the oxidized forms of hemerythrin show three major features (Figure 3). The first of these, at ca. 1.6–1.7 Å (not corrected for phase shift), is the result of Fe–O/N interactions. The Fe···Fe interaction is primarily responsible for the peak at ca. 3 Å, while nonbonded histidine C/N atom interactions with the metal give rise to the last feature at 3.5–4.0 Å. The first attempts to fit the EXAFS data of the oxidized Hr complexes gave iron–ligand separations in excellent agreement with the X-ray diffraction results; however, Fe···Fe distances were overestimated by ~0.15–0.25 Å relative to the crystal structures.[36,37] More recent studies using better synthetic complexes as models (see section VII) have resulted in fits that gave Fe···Fe separations in excellent agreement with the X-ray diffraction results[40] (Table II). In the Fourier transform of the EXAFS data of deoxyHr, the middle feature is much reduced in intensity and shifted to a longer distance, indicative of an increase of ≥0.3 Å in the Fe···Fe separation.[40] Thus, reduction to the deoxy level results in loss of the short iron–oxide bonds, probably due to protonation of the bridging oxo group. Fits to the difference in the EXAFS between deoxyHr and oxyHr indicate that reduction from the oxy to deoxy level results in release of O_2 and lengthening of the bonds to the bridging ox-

TABLE II. Results of Fits to the EXAFS of Various Forms of Hemerythrin (Ref 40)

source	Fe–O_{oxide} no.	Fe–O_{oxide} R, Å	Fe–O no.	Fe–O R, Å	Fe–N no.	Fe–N R, Å	Fe···Fe: R, Å
$metN_3$	1.0 (3)	1.80 (3)	2. 0 (4)	2.08 (4)	3.0 (5)	2.17 (4)	3.24 (5)
met	1.0 (3)	1.82 (3)	2.0 (4)	2.07 (4)	2.5 (5)	2.14 (4)	3.13 (5)
oxy	1.0 (4)	1.82 (3)	2.5 (5)	2.11 (4)[a]	2.5 (6)	2.22 (4)[a]	3.24 (5)
deoxy	1.0 (4)	1.98 (4)	2.4 (6)	2.12 (6)[a]	2.5 (6)	2.5 (6)[a]	3.57 (6)
$semimetN_3$[b]	0.5	1.87	2.5	2.135[a]	3.0	2.135[a]	3.46

[a] N and O contributions could not be distinguished. [b] Reference 39.

ygen.[40] A lengthening of the Fe–oxide and Fe···Fe distances relative to $metN_3Hr$ by ~0.07 and 0.28 Å, respectively, is also observed for $semimetN_3Hr$.[39]

The energies of the X-ray absorption edge of oxyHr and the various met forms of Hr are consistent with both irons being trivalent.[36,37] In contrast, the edge energy for deoxyHr is shifted to lower energy relative to its counterparts, suggesting that both irons in this form are divalent.[36]

These oxidation state assignments are consistent with Mössbauer spectroscopic results.[41-45] Mössbauer spectra of deoxyHr reveal a single quadrupole doublet with a large isomer shift (δ = 1.14 mm/s) and quadrupole splitting (ΔE_Q = 2.76 mm/s) at 4.2 K, indicative of high-spin Fe(II) (probably with N and O ligands) (Figure 4); thus, the two irons are indistinguishable. OxyHr gives rise to a spectrum consisting of two quadrupole doublets with similar isomer shifts (δ = 0.51, 0.52 mm/s) but different quadrupole splittings (ΔE_Q = 0.91, 1.93 mm/s).[41-45] Each doublet accounts for half of the signal, and the spectrum is not broadened by application of a magnetic field. These results are consistent with the presence of two high-spin ferric ions that are antiferromagnetically coupled (making the dinuclear center diamagnetic) but which experience different electric field gradients. The Mössbauer parameters of oxyHr are strikingly similar to those of synthetic oxide-bridged dinuclear iron complexes[41] (section VII). The spectra of $metN_3Hr$ consist of two very similar quadrupole doublets (ΔE_Q = 1.95, 1.47 mm/s), with isomer shifts of 0.51 mm/s similar to those of oxyhemerythrin;[44] the data again indicate the presence of two high-spin ferric ions that are antiferromagnetically coupled.

Magnetic-susceptibility measurements on the oxidized forms of Hr confirm that the two ferric ions are antiferromagnetically coupled.[41,42,46,47] Variable-temperature results using a SQUID magnetometer gave exchange coupling constants (J) between the $S = {}^5/_2$ ferric ions of −77 and −134 cm^{-1} for oxyHr and metHr[47] (using the spin Hamiltonian $H = -2J\tilde{S}_1\cdot\tilde{S}_2$).[48] Such large negative exchange constants have been observed only for synthetic diiron complexes containing a bridging oxo ligand (section VII). Measurements at room temperature on deoxyHr gave magnetic moments per iron in the range expected for isolated ferrous (S = 2) centers,[42] with no evidence for magnetic coupling of the iron atoms (but see discussion of MCD and EPR spectra of deoxyHr below).

The first ^1H NMR studies of $metN_3Hr$ revealed that signals from four histidine residues of the apoprotein were broadened beyond detection in the iron complex because of their proximity to the iron centers;[49] the discrepancy between the observed number of iron-bound histidines and the five expected based on the crystallographic studies could not be explained. Recently ^1H NMR studies of the various paramagnetic forms of Hr have been used to identify the ligands to the diiron complex.[50,51] For oxy and metHr, three or four resonances, exchangeable with D_2O, were observed in the 12–25 ppm region and assigned to imidazole N–H protons.[51] The decreased magnitude of the isotropic shifts compared to those of mononuclear iron(III)–imidazole complexes (ca. 100 ppm) results from antiferromagnetic coupling between the irons. A nonexchangeable signal at 11 ppm was assigned to the methylene protons of the bridging carboxylate groups. Three exchangeable resonances between 65 and 40 ppm (assigned to histidine NH protons) were found in the

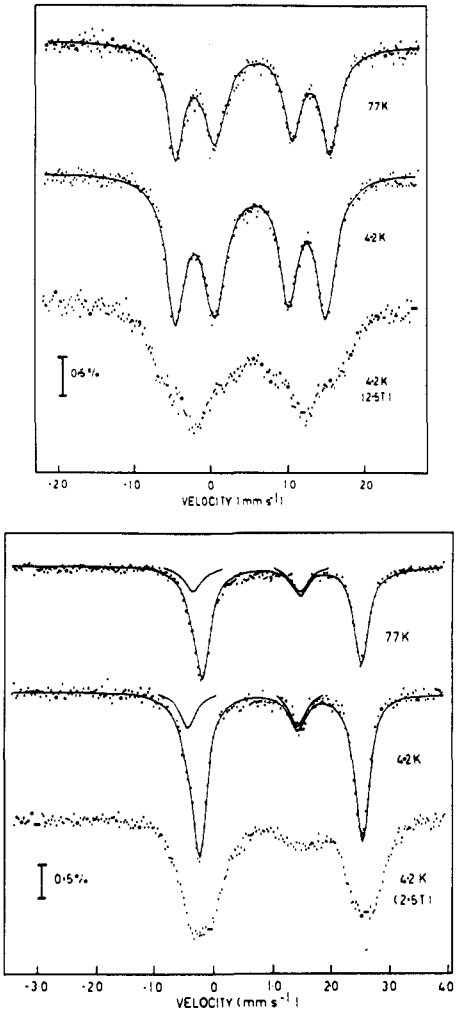

Figure 4. Mössbauer spectra of oxyhemerythrin (top) and deoxyhemerythrin (bottom) at temperatures of 77 and 4.2 K and in a magnetic field of 2.5 T at 4.2 K. The deoxy spectrum contains contributions from a small amount of the oxyhemerythrin form (reprinted from ref 44; copyright 1984 American Chemical Society).

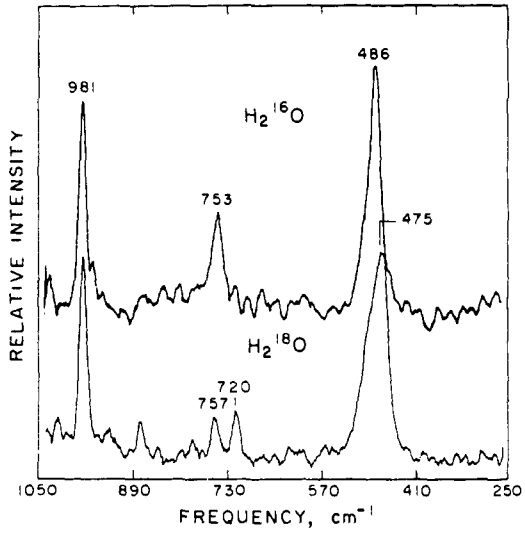

Figure 5. Resonance Raman spectra of oxyhemerythrin with ^{16}O or ^{18}O bridging ligands obtained with 363.8-nm excitation (reprinted from ref 63; copyright 1984 American Chemical Society).

spectrum of deoxyHr, in addition to numerous other paramagnetically shifted signals. An exchange coupling constant of $J \approx -15$ cm^{-1} was determined by Evans susceptibility measurements for deoxyHr.[51] Addition of anions known to bind to deoxyHr resulted in weakening of the antiferromagnetic coupling. SemimetN_3Hr gave rise to two sets of histidine NH resonances near 72 and 54 ppm, assigned to histidines bound to the Fe(III) and to the Fe(II), respectively.[51] These data would suggest that a trapped valence description is most appropriate for the iron ions of semimetN_3Hr (at least on the NMR time scale). The temperature dependence of the isotropic shift of semimetN_3Hr gave an exchange value of $J \approx -20$ cm^{-1}.

As deoxyHr contains two Fe(II)'s and each Fe center is oxidized to the trivalent state upon the binding of dioxygen, the dioxygen unit must undergo a two-electron reduction to peroxide. Resonance Raman studies of oxyHr[52-56] have unequivocally established that the oxidation level of the bound O_2 is peroxide (O_2^{2-}). Excitation into a charge transfer band at 500 nm (vide infra) resulted in peaks assigned to Fe–O_2 and O–O stretches at 503 and 844 cm^{-1}, respectively.[52] These assignments were confirmed on the basis of the observed shifts with $^{18}O_2$. The O–O stretch at 844 cm^{-1} clearly identifies the bound form of O_2 as peroxide. Use of ^{16}O–^{18}O clearly showed that the two oxygens of the peroxide were inequivalent, indicating that the peroxide was not bound in a symmetrical fashion.[54] Similar studies with metN_3Hr using $^{15}N^{14}N_2^-$ revealed an inequivalence of the two end nitrogens.[54] Resonance Raman studies have also provided additional evidence for the presence of an oxo bridge.[56,58-61] Peaks at ~510 and 750–785 cm^{-1} for metHr's (which shift ~15 and ~35 cm^{-1} to lower energy in the presence of $H_2{}^{18}O$) have been assigned to ν_s(Fe–O–Fe) and ν_{as}(Fe–O–Fe), respectively. However, for oxyHr, the ν_s(Fe–O–Fe) and ν_{as}(Fe–O–Fe) occur at lower frequencies, 486 and 753 cm^{-1}, respectively (Figure 5). This has been attributed to the presence of a hydrogen bond to the oxo bridge[61] and is supported by a shift in both ν_s(Fe–O–Fe) and ν_{as}(Fe–O–Fe) to higher frequency in D_2O. The resonance Raman spectra of semimetN_3Hr are distinct from those of oxidized Hr's in that the ν_s(Fe–O–Fe) stretch

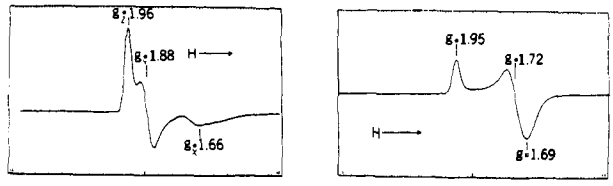

Figure 6. EPR spectra of $(semimet)_R$ (left) and $(semimet)_O$ hemerythrin (right) from *Themiste zostericola* (reprinted from ref 14; copyright 1980 Elsevier).

is not observable.[62] The unique pH dependence of metHr has been examined by resonance Raman techniques;[63] in the basic form of the protein, the open coordination site of the five-coordinate iron is filled by a hydroxo ligand as shown by an Fe–O stretch at 490 cm^{-1} (shifted to 518 cm^{-1} in D_2O). (This form of the protein is thus best termed methydroxyHr.)

Resonance Raman experiments have also proved valuable in assigning the electronic spectra of the various forms of Hr. Oxidized Hr's all display four bands at 320–340 (ϵ = 6000–7000), 360–380 (~4000–6000), 440–410 (~500–950), and 590–750 nm (~140–200).[64] Fe–O–Fe stretches are maximally enhanced in the resonance Raman spectra by excitation at ca. 380 nm, indicating the band at 360–380 nm possesses significant oxide → Fe(III) charge-transfer contributions. Similarly excitation in the 440–510-nm bands also show some enhancement of the Fe–O–Fe bands.[56] The visible bands of oxyHr, metN_3Hr, and metNCSHr, at 500, 446, and 452 nm, respectively, are readily assigned as ligand (O_2^{2-}, N_3^-, NCS^-) to metal charge-transfer bands as a result of their intensities. Polarized single-crystal spectroscopy studies of oxyHr and metN_3Hr indicate that the peroxide and azide ligands have orientations consistent with the X-ray crystallogrpahic results.[65] Recently, visible and near-IR spectra of metN_3Hr and metOHHr have revealed that the bands at ~480 and 600–750 nm and a newly discovered band at ~1000 nm are ligand field transitions of the octahedrally coordinated ferric centers.[66] Electronic spectra of semimetHr are similar to those of their met counterparts, but less distinctive.[67] The N_3^- → metal charge transfer band is retained in semimetN_3Hr, indicating that the endogeneous monodentate binding site is on the ferric center. Bands with intervalence character have been identified in the near-IR spectra of the semimet form.[66]

Both $(semimet)_R$Hr and $(semimet)_O$Hr display EPR spectra at liquid He temperatures (Figure 6); the two spectra are slightly different, with g values of 1.96, 1.88, 1.67, and 1.95, 1.72, 1.68, respectively.[13,14] Addition of azide to either results in a slightly different signal with g values of 1.94, 1.85, and 1.57; the amplitude of the signal does not decrease with time, indicating that the N_3^- adduct is stable to disproportionation. The EPR signals are strikingly similar to those of mixed-valence [2Fe-2S] proteins containing one ferric iron and one ferrous iron.[68] A theoretical model for analyzing the g values of the EPR signals of the semimet forms of Hr indicates that a very small difference in the rhombic distortion of the ferrous site could account for the differences in the spectra.[69]

Finally magnetic circular dichroism and EPR studies on deoxyHr indicate that this form of the protein contains one five-coordinate and one six-coordinate divalent iron antiferromagnetically coupled with $-J \approx 12$–38 cm^{-1}.[70,71] Addition of anions such as azide to the five-

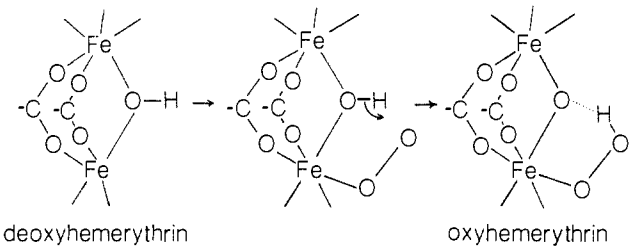

Figure 7. Proposed mechanism for conversion of deoxyhemerythrin to oxyhemerythrin (reprinted from ref 23; copyright 1985 National Academy of Sciences).

coordinate iron results in a significant perturbation of the coupling between the ferrous ions, such that they become weakly *ferro*magnetically coupled. Consequently, these forms give rise to a novel EPR signal at $g \approx 16$ originating from the $|4,\pm4\rangle$ states.

Dialysis of metHr against sulfide results in the generation of another form of semimetHr, in which the oxide (or hydroxide) bridge has been replaced by a bridging sulfide ligand.[72-74] EPR and Mössbauer data indicate that the iron centers remain antiferromagnetically coupled.[73] Recent results indicate that (μ-sulfido)semimetHr can be oxidized by agents such as $Fe(CN)_6^{3-}$ to the (μ-sulfido)metHr species.[74] Generation of the corresponding (μ-selenido)semimetHr has also been described.[73]

A mechanism for the conversion of deoxyHr to oxyHr that is consistent with the spectroscopic and magnetic data on the respiratory protein has been proposed (Figure 7).[23] DeoxyHr possesses the same iron ligation as metHr with the exception of the oxo bridge, which is protonated. As dioxygen approaches the diiron center, it binds to the five-coordinate site. Electron transfer then occurs with oxidation of both ferrous ions to ferric and reduction of the dioxygen to peroxide; this is accompanied by transfer of the hydroxo proton to the peroxide to give a hydroperoxide ion. A scheme showing the interconversion of the various forms of Hr and their probable structures is displayed in Figure 8. In the scheme, the structures of $(semimet)_O$ and $(semimet)_R$ are those proposed recently based on detailed CD and MCD studies.[75] The true picture may be somewhat more complicated, as studies of the equilibrium $(semimet)_R \rightleftarrows (semimet)_O$ indicate that a conformation change is involved.[76]

III. Ribonucleotide Reductase

Ribonucleotide reductase (RR) catalyzes the formation of deoxyribonucleotide di- or triphosphates, the first step in DNA synthesis.[5] Three types of RR have been identified, each possessing a different metal cofactor: one requires adenosylcobalamin (vitamin B_{12}); the second, iron; and the last, manganese.[77] The iron enzyme has been found in animals, certain bacteria, and virus-infected mammalian cells. The enzyme from *Escherichia coli* is the best characterized and will be the focus of this discussion; available data on other iron-containing systems are generally consistent with the results obtained on the *E. coli* enzyme. The enzyme from *E. coli* is composed of two nonidentical proteins in a 1:1 ratio. Protein B1 (160 kDa MW) possesses the two ribonucleotide binding sites and contains redox active dithiol groups. Two identical 39-kDa subunits comprise protein B2; each contributes a tyrosyl radical[78]

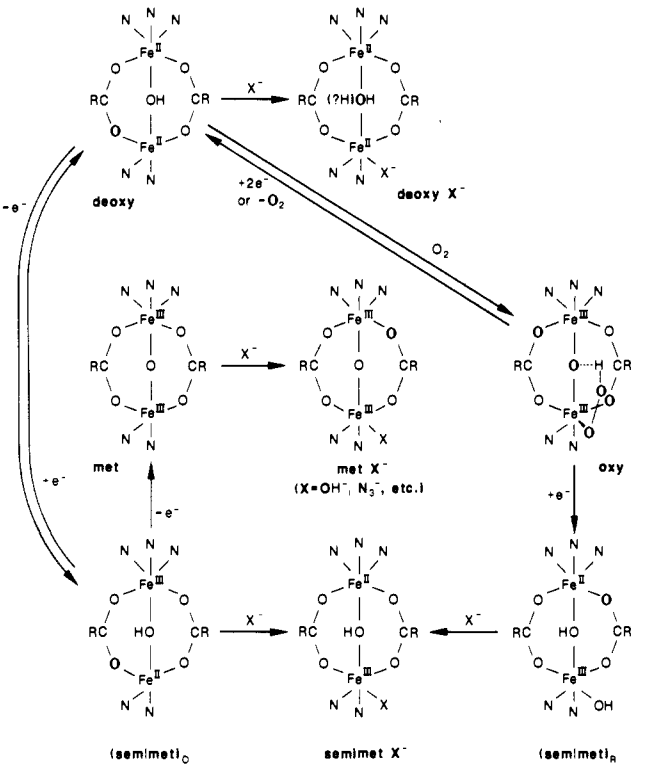

Figure 8. Interconversion of the various forms of hemerythrin.

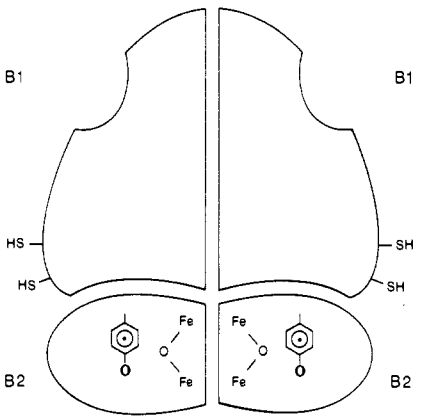

Figure 9. Schematic of *E. coli* ribonucleotide reductase.

and binds non-heme iron, both of which are essential for activity (Figure 9).

While for many years the B2 protein was believed to bind two iron atoms in a dinuclear site (vide infra) at the interface of its two identical subunits,[5] recent investigations have shown that the protein contains a total of four atoms of iron. Consequently, each subunit appears to possess a dinuclear iron center.[78] The spectroscopic properties of these diiron centers are strikingly similar to those of the oxo-bridged diiron units of hemerythrin.

While X-ray diffracting crystals were first reported in 1984,[79] the three-dimensional structure of the B2 protein has only recently been reported at 2.2-Å resolution.[80] Each B2 protein contains two diiron centers and is comprised of eight α-helices with little β-structure. The diiron unit rests in the center of four of the α-helices, with the Fe···Fe axis *parallel* to the axis of the helices (unlike Hr, in which the Fe···Fe and helix axes are perpendicular). The two iron atoms are separated by ~3.3 Å and are doubly bridged by an oxo

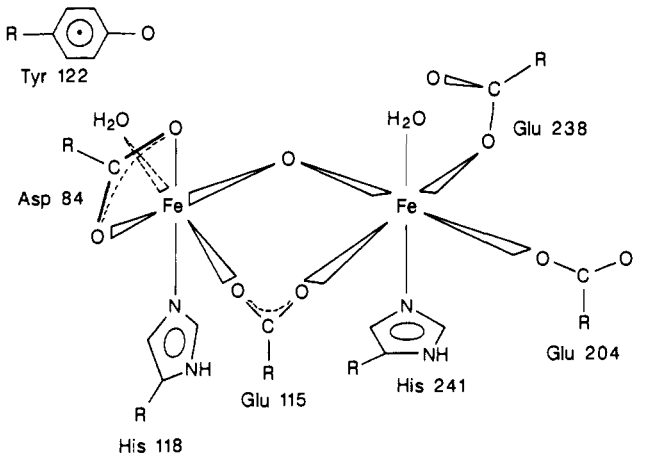

Figure 10. Structure of the diiron site of *E. coli* ribonucleotide reductase (adapted from ref. 80).

ligand and a single glutamate carboxylate ligand (Figure 10). The coordination about each iron is completed by histidine imidazoles, by carboxylate groups from aspartate and glutamate residues, and by water molecules. One carboxylate (Asp 84) binds in a novel bidentate fashion to a single iron. The most intriguing aspects of the structure is that while the irons are only doubly bridged, a second carboxylate group (Glu 238) seems to be in a suitable position to bridge the two irons. These results are also in accord with observed sequence homologies between the iron-containing protein of RR's from a variety of sources.[81] Two of eight histidine residues are conserved between sequences of the enzyme from *E. coli* and the mollusc *Spisula solidissima*, and Epstein Barr and Herpes simplex viruses. A total of eight glutamate and aspartate and two tyrosine residues are also conserved. His 118 (numbers correspond to the *E. coli* sequence), His 241, Glu 115, and Asp 237 or Glu 238 were correctly proposed as iron ligands.[81]

Fourier transforms of the EXAFS data of protein B2 are dominated by two features, resulting from Fe–O/N and Fe···Fe interactions. Fits of the EXAFS data indicated that the iron atoms were coordinated by five or six oxygen and/or nitrogen ligands.[39,82-84] In addition, each iron is bound to an O/N ligand at a short distance of about 1.78 Å, indicative of a bridging oxo ligand. The bond distances to the other ligands average ~2.04 Å, ca. 0.1 Å shorter than that found for Hr; this may reflect the greater number of nitrogenous ligands such as histidine imidazole groups in the latter. This is consistent with fits of a weak third feature in the Fourier transform at ~3.8 Å, which allow for the presence of up to three histidine ligands per diiron unit. The Fe···Fe separation has been reported to be 3.22[39] and 3.26–3.48 Å,[83] depending upon how multiple scattering effects are compensated for in the fits. The similarity in the Fe–O_{oxo} distance and Fe···Fe separation for RR and Hr suggested that the diiron centers of the B2 protein might also possess a triply bridged core, perhaps with one bridging oxo group and two bridging carboxylates (although this was not confirmed by the X-ray structure). Addition of hydroxyurea (which reduces the tyrosine radical) had no effect on the EXAFS spectra.[39,83]

Mössbauer spectra of ^{57}Fe-reconstituted protein revealed two pairs of quadrupole doublets of approximately equal intensity,[78,85] indicating the presence of two inequivalent sets of iron. The quadrupole splitting and chemical shifts of the doublets are typical of high-spin ferric iron with oxygen- and nitrogen-based ligation (δ = 0.53, 0.45 mm/s, ΔE_Q = 1.65, 2.45 mm/s at 4.2 K).[85] At low temperature, no magnetic features were observed even in strong applied magnetic fields; thus, the iron sites are diamagnetic, meaning that the two irons are antiferromagnetically coupled.[85] Addition of hydroxyurea resulted in no observable changes in the Mössbauer spectra. However, reduction of the protein with dithionite or the addition of ferrous iron to the apoprotein resulted in a significantly different spectrum with parameters typical of Fe(II) (δ = 1.26 mm/s, ΔE_Q = 3.13 mm/s at 4.2 K).[78] Sizeable hyperfine interactions were observed in the presence of strong magnetic fields; preliminary analysis suggested that the magnetic coupling (J) between the two irons was smaller than the iron zero field splitting (D).

Variable-temperature magnetic susceptibility studies also indicate that the two irons are strongly antiferromagnetically coupled, with a coupling constant J of -108 cm^{-1}.[86] ^{1}H NMR spectra of the B2 protein reveal two paramagnetically shifted resonances at 19 and 24 ppm;[87] in D_2O, only the 19 ppm resonance is observed. Reduction of the tyrosine radical resulted in no change in the two resonances. The exchangeable proton at 24 ppm was assigned to an N–H proton of a histidine ligand, on the basis of comparisons with the ^{1}H NMR spectra of Hr. The feature at 19 ppm has yet to be assigned. In the case of dithionite-reduced protein, resonances at 45 and 57 ppm were observed at 37 °C. The 57 ppm resonance was shown to be due to an exchangeable proton and assigned to an N–H proton of a histidine ligand. Fitting the temperature dependence of the 57 ppm resonance gave a magnetic coupling constant of $J = -5 \pm 5$ cm^{-1}. Upon addition of dioxygen, the ^{1}H NMR spectrum of the oxidized form of the protein was observed.[88]

The ultraviolet–visible spectrum of the hydroxyurea-treated B2 protein is quite similar to that of metHr, with bands at 325 (ϵ = 9400), 370 (7200), ~500 (br, sh, 800), and 600 nm (300) (Figure 11). When Tyr 122 (responsible for the tyrosine radical) is changed to phenylalanine by site-specific mutagenesis, an identical ultraviolet–visible spectrum is observed.[89] Upon excitation into the 370-nm electronic transition, an enhanced resonance Raman band is observed at 496 cm^{-1}.[90-92] Exposure to $H_2{}^{18}O$ results in a shift to 481 cm^{-1}; thus, the band results from a Fe–O moiety exchangeable with solvent. The rate constant for the exchange was consistent with a μ-oxo-bridged structure. By comparison to the resonance Raman spectra of Hr, the ^{18}O shift and the lack of a shift to lower frequencies in D_2O indicates that this band arises from a symmetric Fe–O–Fe vibration. For the RR from bacteriophage T4, a band observed at 487 ± 4 cm^{-1} probably arises from the same source.[91] After exposure to $H_2{}^{18}O$, an enhanced band at 731 cm^{-1} was suggested as a candidate for an asymmetric Fe–O–Fe stretch. In $H_2{}^{16}O$, this band is probably obscured by protein tryptophan vibrations.[92] The oxide bridge was suggested to be involved in hydrogen bonding, as ν_s(Fe–O–Fe) shifted 3 cm^{-1} to higher energy in D_2O. From the oxygen isotope dependence, the Fe–O–Fe angle was calculated to be

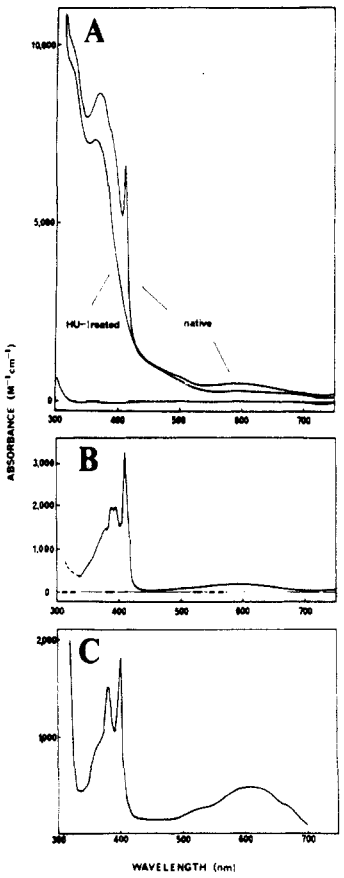

Figure 11. Electronic spectra of *E. coli* ribonucleotide reductase. (A) native protein B2 and hydroxyurea-treated protein, (B) difference spectra of native minus hydroxyurea-treated protein B2, and (C) 2,4,6-tri-*tert*-butylphenoxy radical in hexane (reprinted from ref 86; copyright 1980 Journal of Biological Chemistry).

~138°, suggestive of a di- or tribridged diiron core. A resonance-enhanced band at ~598 cm^{-1}, originally assigned to an Fe–OH stretch,[92] has been reassigned to the symmetric Fe–O–Fe stretch of a photochemically modified dinuclear iron center produced by laser irradiation.[93] RR was shown not to possess any tyrosine ligands to iron, as no phenoxide ring modes were observed.[90]

While the strongly coupled, oxidized form of the B2 protein does not give rise to any observable EPR signals,[93,94] a broad EPR signal at low field similar to that of deoxyN_3Hr has been observed for the dithionite-reduced form of the protein and is indicative of an integer-spin system.[78] However, the possibility that the signal could arise from adventitious Fe(II) could not be absolutely excluded. The temperature dependence of the relaxation rate and line broadening of the EPR signal resulting from the tyrosine radical differed significantly from that of model tyrosine radicals.[95] The difference in the behavior has been suggested to arise from magnetic interactions between the radical and the dinuclear iron centers.

There is no evidence that the dinuclear iron center plays a role in catalysis; instead, it has been proposed that the dinuclear iron center is involved in the generation and stabilization of the tyrosine radical.[85-94] The presence of the radical is known to depend on the presence of iron, and, once reduced (by hydroxyurea, for example) the radical and associated enzymatic activity can only be restored by reduction of the diiron center to the diferrous form and subsequent reoxidation. In the presence of dioxygen, a diferric iron–peroxide complex or an analogous species is proposed to oxidize the tyrosine side chain to generate the tyrosine radical.[88] An oxidoreductase which may be responsible for the reduction to the diferrous form in vivo has been identified.[96-98]

TABLE III. Some Molecular Properties of Various Purple Acid Phosphatases

source	MW, kDa	no. of subunits	metal content[a]	ref
porcine allantoic fluid	35–40	1	2 Fe	99–103
porcine allantoic fluid, high MW form	80	2[b]	2 Fe	104
beef/ox spleen	40	2[b,c]	2 Fe	105–109
rat bone	40	1	1.3 Fe	110
rat spleen	33	1	2 Fe	111
human osteoclastoma	30	1	4.4 Fe	112
human spleen	34	1	2 Fe	113
sweet potato (Kintoki/Kokei)	55	2	1–2 Mn[d]	114–116
sweet potato (Jewel)	55	2	2 Fe[d]	117
kidney bean	65	2	1 Fe, 1 Zn	118, 119
spinach	92		0.3 Mn	120
soybean	60	4	2 Mn[d]	121, 122
rice plant cell walls	65		Mn	123
Micrococcus sodonesis	80		8 Ca^{2+}	124
Neurospora crassa	85		-	125
Aspergillus ficuum	85		-	126

[a] Per subunit. [b] Nonidentical. [c] Probably two proteolytic fragments (15 and 23 kDa) of a single subunit. [d] Per molecule.

IV. Purple Phosphatases

Purple acid phosphatases (PAP's) are transition-metal-containing glycoproteins that are distinguished by their low pH optima for enzymatic activity, their insensitivity to inhibition by tartrate, and their intense pink or violet coloration. They have been isolated and characterized from a variety of mammalian, plant, and microbial sources. PAP's for which molecular properties have been reported are listed with their sources in Table III. The most extensively characterized purple acid phosphatases, uteroferrin and beef spleen PAP, contain two iron atoms per molecule.[100,127-129] Treatment of the isolated enzymes with mild reductants effects a blue shift in the maximum absorbance from 550 to 510 nm (purple to pink).[108,130,131] Greater variation in the metal ion content has been observed for the plant enzymes, with reports indicating the presence of iron, manganese, and zinc ions. Although metal analyses have not been reported for the microbial enzymes, their violet color and enzymatic properties strongly resemble those of the other PAP's.

Despite substantial efforts in several laboratories, crystals suitable for high-resolution X-ray diffraction studies have not been obtained for any purple acid phosphatase. Thus, no direct information on the tertiary structure of these enzymes is available. There is, however, a growing body of information on the primary sequences of these enzymes, as well as spectroscopic data that has been correlated to secondary structural features.

Amino acid sequences for beef spleen purple acid phosphatase (determined by conventional sequencing techniques), uteroferrin (determined conventionally and from the cDNA sequence), and human tartrate resistant acid phosphatase (TRAP) (determined from the cDNA

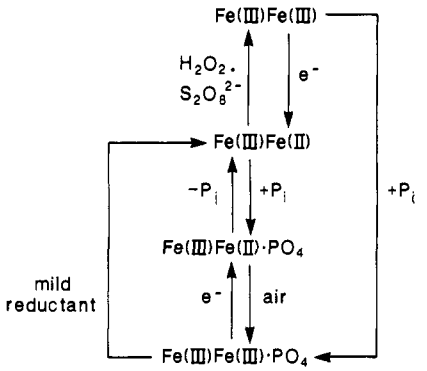

Figure 12. Interconversion of oxidized and reduced species of purple acid phosphatases in the presence and absence of phosphate.

sequence) show greater than 90% homology.[132-134] The absence of repetitive sequences of tyrosine and histidine residues in identical spatial relationships supports the spectroscopic evidence (vide infra) that the metal atoms are coordinated asymmetrically by these ligands. Homology has been observed between the mammalian purple acid phosphatases and the phosphoprotein phosphatases 1, 2A, and 2B for the residues 186 to 237 and 51 to 103, respectively (numbering schemes based on human TRAP[133] and rabbit PP2Aα[135]). These regions contain a large number of potential metal binding amino acid residues.[136]

Circular dichroism spectra of the far-UV (200–250 nm) region of uteroferrin indicate secondary structure containing 17% α-helix, 9% β-helix, and 74% random structure for the purple form; 18% α-helix, 11% β-pleated sheet, and 71% random structure for the pink form; and, for the purple phosphate complex, 12% α-helix, 6% β-pleated sheet, and 82% random structure. The spectra of the aromatic (250–300 nm) and near-UV–visible regions (300–600 nm) also show little difference between the purple and pink forms. However, upon addition of phosphate to the purple form, an additional band appears around 340 nm.[101,137]

The property that most readily distinguishes the purple acid phosphatases is their violet color. Curiosity about this unusual chromophore has prompted extensive spectroscopic investigation, including UV–visible, Mössbauer and magnetic resonance spectroscopies, and magnetic susceptibility studies. Since the most detailed of these studies have been performed on the beef spleen and porcine enzymes, they will be the focus of the following discussion. The interconversion of the oxidized and reduced species of uteroferrin and beef spleen PAP in the presence and absence of phosphate is shown in Figure 12.

The absorbance maxima for the oxidized (purple) and reduced (pink) forms of the enzyme are 550 and 510 nm, respectively, with ϵ = 2000 M^{-1} cm^{-1} per Fe in either form at pH 6 (Figure 13).[107,108,138-141] However, the phosphate complex of the reduced enzyme exhibits a highly pH dependent absorption maximum, with λ_{max} ranging from 561 to 530 nm between pH 3 and 6,[139,140] in contrast to reduced enzyme whose spectrum is virtually pH independent. All spectra also exhibit a protein absorbance at 280 nm with a broad shoulder near 310 nm.

Beef spleen PAP is usually isolated as the oxidized purple enzyme–phosphate complex, in which both iron atoms are in the ferric oxidation state and which con-

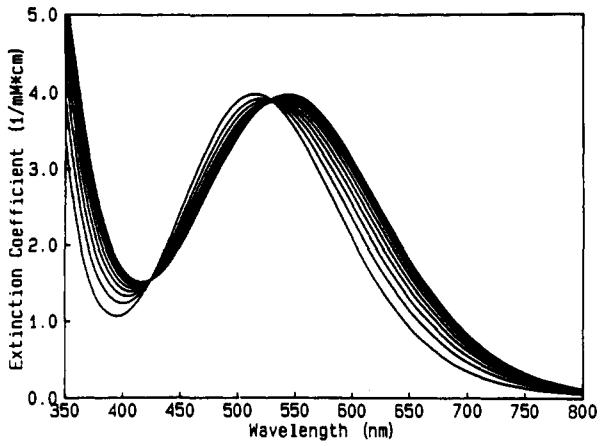

Figure 13. The conversion of reduced uteroferrin to the oxidized phosphate complex in the presence of 9 mM phosphate at pH 6, monitored by optical spectroscopy (reprinted from ref 139; copyright 1986 Journal of Biological Chemistry).

tains a single tightly bound phosphate ion.[108,138] Exposure to mild reductants, such as ascorbate or dithioerythritol,[108,130,138] yields the pink form in which one of the iron ions is reduced; this is the form in which uteroferrin from allantoic fluid is usually obtained. Addition of phosphate to the pink form under anaerobic conditions produces a phosphate complex of the reduced enzyme,[139] which is gradually oxidized in the presence of oxidants, such as air, to the oxidized purple enzyme–phosphate complex (Figure 13). Addition of phosphate directly to the oxidized enzyme yields the same purple complex.[139,142] Rigorous conditions, such as hydrogen peroxide or ferricyanide oxidation, are required for conversion of the reduced pink form to the oxidized purple form in the absence of phosphate.[3,100,142] Preliminary electrochemical studies on uteroferrin have determined the potential for the one-electron reduction of purple oxidized enzyme to pink reduced enzyme to be ~320 mV.[143] High molecular weight uteroferrin (Table III) is isolated primarily in the active reduced form. Apparently the presence of the additional noncatalytic subunit protects the enzyme against oxidation during purification. Considerable controversy has surrounded the identification of a reduced phosphate complex,[139,141,142,144,145] and spectroscopic evidence to support its existence has only recently been obtained (vide infra).

Fe EXAFS data for the oxidized phosphate complex of beef spleen PAP[146] and uteroferrin[5] indicate a short iron–iron distance (3.0 or 3.2 Å, respectively), consistent with the presence of multiple bridging ligands. In addition, the data suggests the presence of two sets of O/N scatterers, three at 1.98 Å and three at 2.13 Å from the iron atoms, and an Fe···P distance of 3.06 Å, indicating direct coordination of phosphate to at least one of the iron atoms in the purple phosphate complex. An enhanced peak indicating an Fe–C/N distance of 4.3 Å suggests coordination of a histidine imidazole, as seen in hemerythrin. No evidence for a bridging oxide was observed. Fits of the EXAFS data measured on the pink form indicate the same overall coordination number for the iron sites, but only two short O/N distances rather than three or four as observed in the purple form. No peak attributable to an Fe···Fe interaction was observed in the EXAFS of the pink form, suggesting that loss or protonation of a bridging oxide atom has oc-

TABLE IV. ^{57}Fe Mössbauer Data for Purple Acid Phosphatases and Their Phosphate Complexes

form	δ (ΔE_Q)[a] Fe_A	Fe_B	T, K
Fe(III)-Fe(III)	0.55 (1.65)	0.46 (2.12)	10[b]
Fe(III)-Fe(III)·PO_4^{3-}	0.52 (1.02)	0.55 (1.38)	4.2[c]
	0.51 (1.03)	0.54 (1.36)	4.2[d]
	0.52 (0.90)	0.58 (1.40)	77[e]
Fe(III)-Fe(III)	1.17 (2.65)	0.67 (1.27)	77[e]
	0.52 (1.83)	1.27 (2.66)	100[b]
	0.53 (1.78)	1.22 (2.63)	119[c]
Fe(III)-Fe(II)·PO_4^{3-}	0.54 (0.78)	1.23 (2.76)	119[c]

[a] In mm/s. [b] Reference 147. [c] Reference 139. [d] Reference 148. [e] Reference 149.

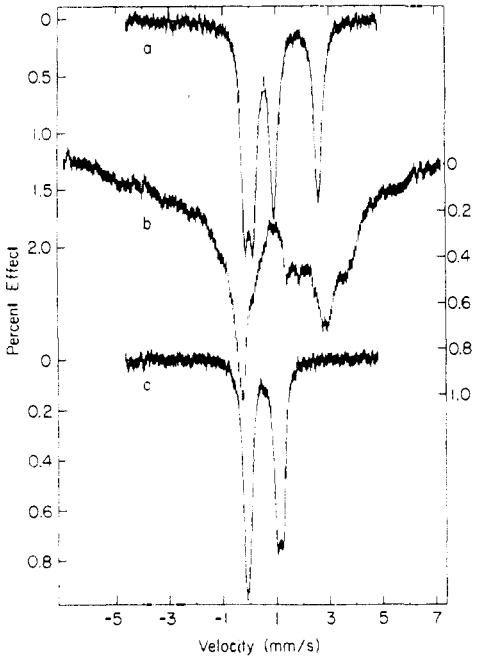

Figure 14. Mössbauer spectra of the phosphate complex of reduced uteroferrin at (a) 119 K and (b) 4.2 K in a field of 170 mT perpendicular to the γ-beam and (c) oxidized uteroferrin phosphate complex at 4.2 K (reprinted from ref 139; copyright 1986 Journal of Biological Chemistry).

curred with significant lengthening of the Fe···Fe distance, as in deoxyhemerythrin. Near-edge features in the X-ray absorption spectrum suggest that the Fe coordination geometry is pseudooctahedral or seven coordinate, while a shift of the absorption edge to lower energy for the pink form is consistent with reduction of one of the irons from ferric to ferrous.

Mössbauer spectroscopy and magnetic susceptibility studies have demonstrated the presence of an antiferromagnetically coupled iron center in the oxidized and reduced enzymes and their phosphate complexes. The parameters for the individual species are compiled in Table IV. For the ^{57}Fe-enriched oxidized purple form of uteroferrin, the isomer shifts and quadrupole splittings indicate two distinct high-spin ferric centers that are antiferromagnetically coupled, as implied by the lack of magnetic hyperfine splitting in spectra obtained at 4.2 K (Figure 14).[147] The unusually large quadrupole splittings suggest strong distortions from octahedral symmetry and are comparable to those observed for hemerythrin. The isomer shifts and quadrupole splittings of the oxidized phosphate complex of beef spleen PAP and uteroferrin are also consistent with the presence of two high-spin ferric centers, but the parameters are distinct from those obtained in the absence of phosphate.[139,148,149] The parameters for the pink reduced enzyme are similar for uteroferrin and the beef spleen enzyme and indicate the presence of an antiferromagnetically coupled Fe(II)-Fe(III) center. Again, the parameters for the phosphate complex of reduced uteroferrin are consistent with this assignment but distinct from those of the phosphate-free reduced enzyme.[139]

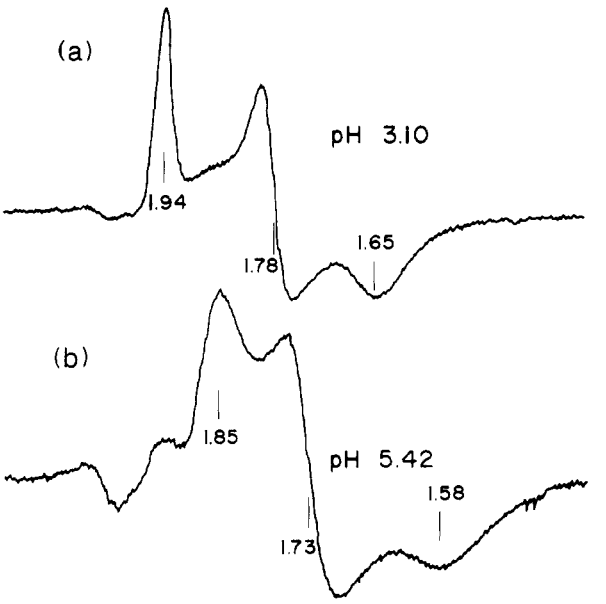

Figure 15. X-band EPR spectra of pink (reduced) beef spleen PAP at (a) pH 3.10 and (b) pH 5.42 at 6.7 K (reprinted from ref 148; copyright 1987 American Chemical Society).

Magnetic susceptibility studies using various techniques have provided estimates of the antiferromagnetic spin coupling constants, J. For the oxidized purple form, values of $-J$ of ≤ 40[128,150,151] and ≤ 150 cm^{-1} [148] have been reported, indicating the presence of strong antiferromagnetic coupling. For the pink reduced enzyme, values of $-J$ ranging from 5 to 11 cm^{-1} have been reported[144,148,150] and, for the reduced phosphate complex,[144] $-J = 3.0$ cm^{-1}. Despite the range of values for the magnetic coupling, it is apparent that the iron ions in the dinuclear center are more strongly coupled in the purple oxidized enzyme than in the reduced forms. The magnitude of the antiferromagnetic coupling observed for the dinuclear iron centers in the PAP's can be explained by the presence of a bridging oxide, possibly supported by additional bridging ligands, between two unsymmetrical iron centers, with protonation of the oxide upon reduction.

The pink reduced forms exhibit a pH-dependent, rhombic EPR signal at temperatures less than 30 K that double integrates to one spin per two iron atoms (Figure 15).[101,147] The signal results from a mixture of two species: a low pH form with $g = 1.94$, 1.78, and 1.65 and a high pH form with $g = 1.85$, 1.73, and 1.58, related by an apparent pK_a of ca. 4.4.[148] The resemblance of this spectrum to that observed for semimethemerythrin suggests that it arises from an antiferromagnetically coupled, oxo-bridged dinuclear iron center with an $S = {}^1/_2$ spin state. Linear electric field effect (LEFE) studies indicate that this paramagnetic center is noncentrosymmetric, suggesting that the charge is localized on one of the iron atoms.[156] Exchangeable protons have

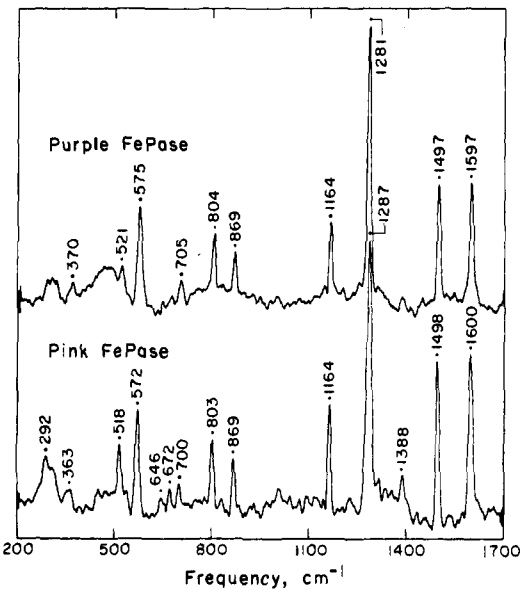

Figure 16. Resonance Raman spectra of 5 mM purple (top) and 2.7 mM pink (bottom) forms of beef spleen PAP at 5 °C in 10 mM NaOAc buffer, pH 5.0, using 514.5-nm excitation (reprinted from ref 148; copyright 1987 American Chemical Society).

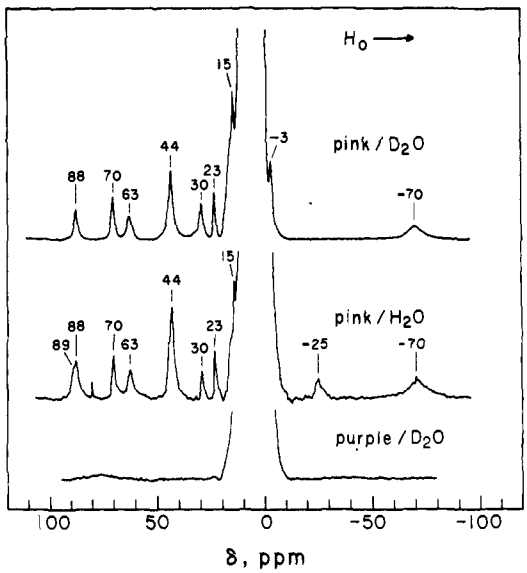

Figure 17. 300-MHz ^{1}H NMR spectra of pink and purple uteroferrin (1 mM) at pH 4.9 and 30 °C (reprinted from ref 150; copyright 1983 Journal of Biological Chemistry).

also been observed in the ^{1}H ENDOR spectra of uteroferrin–molybdate complex (vide infra). Analysis and assignment of the EPR spectrum was initially confused by reports that uteroferrin contained only one iron per protein,[102,127,129,152,153] and that the EPR signal was observed for both pink and purple forms of the enzyme.[129,152] Absence of an EPR signal at low temperatures in samples of the oxidized purple enzyme supports the presence of a antiferromagnetically spin-coupled dinuclear center.

Resonance Raman spectra (Figure 16) using visible excitation show four resonance-enhanced tyrosine ring modes between 1650 and 1150 cm^{-1} for metalloproteins containing tyrosinate residues as ligands. Bands at 1597, 1497, 1281, and 1164 cm^{-1} are observed in the spectra of the purple form of the beef spleen enzyme.[148] The only significant changes observed in the spectrum of the pink form are a shift of the 1281 cm^{-1} band to 1287 cm^{-1} and an increase in the intensity of a 520 cm^{-1} feature.[148] The same general features, including the changes upon reduction, have been observed for uteroferrin.[137,154] In addition, low-frequency excitation of either protein produces bands at 870 and 806, and 574 cm^{-1}, which have been attributed to a metal-coordinated tyrosyl Fermi doublet and to a combination mode with a significant Fe–O stretching contribution, respectively.[137] No evidence for the Fe–O–Fe symmetric stretch at ~500 cm^{-1} that is observed in spectra of hemerythrin and ribonucleotide reductase is present in spectra of uteroferrin or beef spleen PAP. Enhancement of this mode in complexes containing unsaturated nitrogen ligands trans to the oxo group has been observed,[155] and a histidine imidazole ligand occupies this position in hemerythrin (but not in ribonucleotide reductase). Absence of such a ligand trans to the oxo group in the PAP's may explain the absence of this feature in their spectra, but the factors governing enhancement of the Fe–O–Fe symmetric stretch remain to be defined in detail.[155]

Comparison of the ^{1}H NMR spectra of dinuclear model compounds and those of reduced uteroferrin (Figure 17) suggests that resonances found at −70, 44, and 63 and 70 ppm arise from ortho-, β-methylene and two meta protons of tyrosinate ligands, respectively. Exchangeable protons that have been assigned to histidine imidazoles are seen at 44 and 89 ppm. In addition, an exchangeable proton signal of uncertain origin is observed at −25 ppm.[150] Evidence for nitrogen ligation is also present in the ENDOR and electron spin echo spectra.[156,157]

The results of X-ray absorption, resonance Raman, and NMR studies together with the small change that is observed in the extinction coefficient of the A_{550}/A_{510} band in the visible spectrum suggest that the dinuclear iron centers of uteroferrin and beef spleen PAP are coordinated by at least one tyrosinate ligand on the nonreducible iron, that histidine imidazole is a probable ligand to both irons, that the presence of a carboxylate bridge(s) analogous to those found in hemerythrin and ribonucleotide reductase is likely, and that phosphate is coordinated to the iron center in the oxidized purple phosphate complex. Plausible structures for the dinuclear iron centers in the PAP's based on the available spectroscopic evidence are shown in Figure 18.

Several studies have been undertaken to correlate the loss of activity with the shift in λ_{max} upon addition of phosphate to the reduced enzyme. Phosphate is a competitive inhibitor of the reduced enzyme, with $K_i \approx 3$ mM. Attempts to utilize spectroscopic studies on the reduced enzyme–phosphate complex to infer the mode of substrate binding have been complicated by its peculiar spectroscopic properties and by the tendency of phosphate to induce oxidation of the iron center. Early results suggested a rapid, reversible binding of phosphate to reduced enzyme followed by a slow oxidation and loss of activity.[142] Later studies failed to detect the equilibrium complex by EPR, and parallel loss of activity and shift of λ_{max} were observed, suggesting that rapid oxidation occurs upon phosphate binding.[141,145] Formation of the reduced phosphate complex was conclusively demonstrated by Mössbauer spectroscopy,[139] and recently its EPR spectrum has been reported.[144] At 8 K the reduced uteroferrin–phosphate complex exhibits a broad EPR signal with

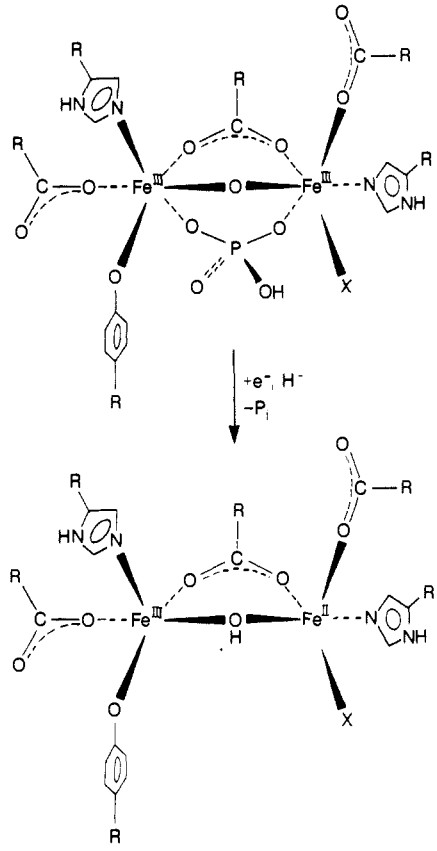

Figure 18. Proposed active site structure of purple acid phosphatases.

g = 2.27, 1.51, and 1.06 that is very difficult to detect under the conditions used to detect (Figure 15) uncomplexed reduced enzyme, possibly explaining the discrepancies in earlier reports regarding phosphate binding.

In addition to phosphate, several inhibitors of reduced uteroferrin significantly alter its optical and magnetic properties. The phosphate analogues, arsenate, vanadate, and molybdate, have been studied most extensively, and the results of their effects are compiled in Table V. Addition of any of these tetrahedral oxyanions results in a shift in the maximum absorbance in the visible spectrum of the enzyme. Vanadate causes disappearance of the EPR signal, which is accompanied by the appearance of a new signal characteristic of the vanadyl ion, VO^{2+}, indicating that vanadate has oxidized the enzyme.[159] Arsenate causes broadening and a decrease in intensity of the signal, and molybdate results in an unusual axial signal distinct from, but, with an average g' value of 1.74, comparable to that of reduced uteroferrin. Electron spin echo and ^{95}Mo ENDOR spectroscopic studies of reduced uteroferrin exhibit a hyperfine interaction of a single species of ^{95}Mo molybdate with the $S = {}^1/_2$ Fe(II)–Fe(III) center.[157] Other perturbants include pyrophosphate, which appears to interact analogously to phosphate; fluoride and sulfate, which effect shifts in the absorption maximum and puzzling changes in the EPR spectra; and guanidine, which presumably causes partial unfolding of the protein.[159]

The plant and microbial enzymes are not as well-characterized as the mammalian PAP's. Those for which molecular properties are available are listed in Table III. Sweet potato and kidney bean purple acid

TABLE V. Spectral Properties of Inhibitor Complexes of Purple Acid Phosphatases

inhibitor	K_i, mM	λ_{max}, nm	EPR, g'
arsenate	1.3–2.0[a]	486[b]	1.75[c]
		505–512[a]	1.41, 1.56, 1.92[d]
		530[c]	
vanadate	–	520[c]	–
molybdate	4×10^{-3} [d]	525[d]	1.97, 1.52[c]
	3.7×10^{-4} [e]	515–518[f]	
tungstate	–	515[b]	–
pyrophosphate	–	536[c]	–
fluoride	1.3[e]	540[c]	1.73, 1.63[c]
sulfate	–	505[c]	1.92, 1.75, 1.62 (broadened)[c]
guanidinium·HCl, 3 M	–	525[c]	(broadened)[c]

[a] References 139, 158. [b] Reference 140. [c] Reference 159. [d] Reference 158. [e] Reference 160. [f] References 140, 159.

phosphatases have been spectroscopically characterized to some extent; their metal contents apparently differ from the mammalian enzymes (and possibly from each other). Early reports on the sweet potato enzyme indicated the presence of one manganese ion per dimer of 55-kDa subunits,[116] and later reports from the same laboratory demonstrated that the manganese could be removed and that an iron-substituted enzyme could be prepared, but it exhibited approximately half the phosphatase activity of the native enzyme.[161] In contrast, reports from another laboratory on what appears to be the same enzyme have shown that the sweet potato PAP contains two iron atoms per dimeric protein and that manganese is a contaminant that can be removed with no effect on activity.[117] The kidney bean enzyme is less controversial, with reports indicating the presence of one zinc and one iron atom per 60-kDa subunit in a dimeric enzyme.[119] Statistical comparison of the amino acid compositions of the sweet potato and kidney bean enzymes indicates a high probability of a substantial degree of homology in their sequences,[119,162] but neither sequence has been reported to date.

In contrast to the mammalian PAP's, the plant enzymes are insensitive to mild reductants, and no color change attributable to reduction of the chromophore is observed. Nevertheless their electronic spectra are strikingly similar. The reported values of λ_{max} for the sweet potato PAP range from 515 to 555 nm (ϵ = 2460–3080 M^{-1} cm^{-1}), with a shoulder around 290 nm on the protein absorbance.[114,117,163] The EPR spectrum of the native enzyme from Kintoki potatoes is reported to be featureless, and upon denaturation a six-line signal around g = 2, characteristic of Mn(II) ($I = {}^5/_2$), appeared.[163,164] For the PAP from Jewel potatoes, a high-spin Fe(III) signal similar to the spectrum of kidney bean PAP (vide infra) has been observed.[165] The resonances of $H_2PO_4^-$ and F^- in ^{31}P and ^{19}F NMR spectra, respectively, broaden upon interaction with the enzyme, suggesting interaction of these species with a paramagnetic center.[161,166] Tyrosinate and sulfur ligands to the metal center have been implicated by the resonance Raman spectra,[163,164,167] but spectroscopic studies on synthetic Mn–phenoxide complexes have cast doubt on the presence of sulfur ligands in the sweet potato enzyme.[168]

The kidney bean PAP exhibits a visible absorption spectrum with λ_{max} = 560 nm (ϵ = 3360 M^{-1} cm^{-1})[119] and an EPR spectrum with two signals characteristic of high-spin Fe(III), one with g = 9.22 and 4.28 and the

TABLE VI. Physical Properties of Metal-Substituted Purple Acid Phosphatases

protein	metal	% rel act.	λ_{max}, nm	ϵ/Fe, M^{-1} cm^{-1}	EPR, g'
uteroferrin[a]	Fe-Zn	80	525	3648	-
uteroferrin[b]	Fe-Zn	95	530	2000	4.3, 9.6
uteroferrin[a]	Fe-Cu	25	550	3582	-
beef spleen[c]	Fe-Zn	100	550	2100	4.3
kidney bean[d]	Fe-Fe	154			1.88, 1.76 1.62, 1.49
sweet potato[e] (Kintoki/Kokei)	Fe	38-61	525	3000	4.39

[a] Reference 171. [b] Reference 158. [c] Reference 128. [d] Reference 170. [e] Reference 161 (Reported to contain only one metal ion per subunit.).

other with g = 8.53, 5.55, and 2.85.[169] The number of spins was not quantitated, but these parameters are typical of an $S = {}^5/_2$ spin state as would be expected from an Fe-Zn center.

It has been shown that, under reducing conditions, one of the iron ions in the mammalian PAP's and the zinc ion in the kidney bean PAP are relatively labile, and as a result, methods for metal ion substitution have been developed.[128,131,170] The best characterized metal-substituted PAP's are shown in Table VI together with some of their physical properties. (In addition, an active Fe-Co derivative of kidney bean PAP, Fe-Cd and Fe-Mn derivatives of kidney bean PAP and an Fe-Hg uteroferrin with low activity, and inactive Fe-Cu, Fe-Hg, and Fe-Ni derivatives of the kidney bean enzyme have been prepared.[170,171]) When their labile metal sites are substituted with Zn, uteroferrin and beef spleen PAP exhibit the EPR spectral properties of a center that contains one high-spin Fe(III) ion ($S = {}^5/_2$), strongly resembling the spectrum of the kidney bean PAP.[128,158] Some discrepancy is seen in the extinction coefficients of the visible absorption maxima, which raises a question about the distribution of tyrosinate ligands about the metal center. The kidney bean PAP has been substituted with Fe(II) in the zinc ion site, resulting in an enzyme with activity, redox properties, and an EPR signal analogous to the mammalian PAP's.[169] Iron-substituted sweet potato acid phosphatase has been prepared, and its reported properties are listed in Table VI; however, the nature of the metal center in this enzyme remains controversial, precluding comparison to the other PAP's at this time.

Similar substrate specificities are reported for the mammalian and plant PAP's, but their rates of hydrolysis for various substrates differ. Beef spleen PAP and uteroferrin readily hydrolyze aryl phosphates, di- and trinucleotides, phosphoproteins, pyrophosphate, and a few other activated phosphates.[105,106,138,172-175] The values of K_m and V_{max} for p-nitrophenyl phosphate are 2.0 mM and 580 s^{-1}, respectively,[1-8,170] at pH 6.0 and 22 °C. Alkyl phosphates, mononucleotides, phosphoserine and threonine, and phosphate diesters are hydrolyzed very slowly or not at all.[105,106,138,172-175] The human Gaucher spleen enzyme was shown to be specific for peptide fragments possessing vicinal phosphoserine residues.[176] In contrast to the mammalian PAP's, the plant enzymes preferentially hydrolyze nucleotides, including mononucleotides, rather than aryl phosphates.[115,119,121,161,164] Interestingly, the metal-substituted Fe-Fe kidney bean PAP exhibits only half of the ATPase activity of the native Fe-Zn enzyme, and although K_{cat} for the hydrolysis of p-nitrophenyl phosphate is similar to that of uteroferrin, the Michaelis constant, K_m, is 10-fold lower.[170] The extracellular enzyme from *Micrococcus sodonensis* differs in that it is a purple *alkaline* phosphatase and its substrate specificity is very general, including all substrates mentioned for the mammalian and plant enzymes as well as alkyl phosphates.[124]

The uncertainty that exists regarding the function of the purple acid phosphatases has prompted a number of studies to explore the possibilities. Since uteroferrin is found in such large quantities in allantoic fluid, it has been proposed as an iron transport protein for fetal iron.[177] ^{59}Fe from labeled uteroferrin introduced into the allantoic sacs of live fetal pigs resulted in appearance of ^{59}Fe-labeled transferrin in the allantoic fluid and ^{59}Fe-labeled hemoglobin and other proteins in the fetal liver and spleen.[178] A subsequent EPR spectroscopic study failed to demonstrate significant direct iron transfer from uteroferrin to transferrin under similar conditions,[179] and an alternate role, hydroxyl radical formation by iron-catalyzed Haber-Weiss-Fenton chemistry, has been proposed.[180]

Histochemical and cytochemical studies reveal that the purple phosphatases are localized in the lysosomes of white blood cells and osteoclasts (perhaps even to the inner membrane surface of such organelles).[181-184] In the case of the bovine spleen enzyme, the lysosomes or lysosomelike organelles in which the enzyme accumulates are often associated with aged, deformed erythrocytes,[181] suggesting that the enzyme plays a role in degradation of phosphorylated erythrocyte proteins. The osteoclast enzyme has been shown to be essential for bone-resorption activity.[185]

Lysosomal localization of the purple phosphatases is also supported by the structure of the carbohydrate moieties of uteroferrin from cultured endometrium and of the uteroferrin-associated glycoproteins (noncatalytic subunits) of the high molecular weight uteroferrin, which have been identified as N-linked high mannose oligosaccharides containing 6-phosphomannose units.[104,186,187] In uteroferrin secreted into allantoic fluid, the sixth mannose residue, which is subject to phosphorylation and serves as the lysosomal recognition marker, is absent.[188] The probable glycosylation site is Asn 97, since it is conserved in beef spleen PAP, uteroferrin, and human type 5 acid phosphatase. Asn 128 is another potential site but is conserved only in the latter two. The specific carbohydrate structures of other PAP's have not been reported.

V. Methane Monooxygenase

Methanotrophs are bacteria capable of utilizing methane as their sole energy and carbon source.[189] These organisms oxidize methane to carbon dioxide via CH_3OH, CH_2O, and HCO_2^-. The first and most demanding step of this reaction sequence, the conversion of CH_4 to CH_3OH (eq 1), is catalyzed by the enzyme

$$CH_4 + O_2 + NAD(P)H + H^+ \xrightarrow{MMO} CH_3OH + NAD(P)^+ + H_2O \quad (1)$$

methane monooxygenase (MMO). MMO's are capable of inserting a single oxygen from dioxygen into the C-H bond of a variety of hydrocarbons in addition to the in

TABLE VII. Composition of Methane Monooxygenases

source	*M. capsulatus*[a]	*Methylobacterium*[b]	*M. trichosporium*[c]
component A, $\alpha_2\beta_2\gamma_2$ (hydroxylase/ oxygenase)	210 kDa	220 kDa	245 kDA
α	54 kDA	55 kDa	54 kDa
β	36 kDa	40 kDa	43 kDa
γ	17 kDa	20 kDa	22 kDa
Fe	2.3 (3.3)[d]	2.8	4.3
component B, (regulatory)	16 kDa		15 kDa
component C, (flavoprotein)	42 kDa	40 kDa	39 kDa

[a] References 191, 193, 194. [b] References 197. 198. [c] References 199, 200. [d] Reconstituted; Reference 201.

vivo substrate, methane.[189] Small alkanes are readily oxidized to both primary and secondary alcohols while alkenes are converted to epoxides or other products.

Two types of MMO's have been isolated from these organisms: a membrane-bound, copper-containing enzyme[190] and a soluble, non-heme iron-containing protein (the focus of this discussion); factors which govern the form of the enzyme produced are complex and poorly understood.[189] Methanotrophs themselves are divided into two categories depending on the manner in which carbon is assimilated (via the ribulose monophosphate pathway, type 1, or the serine pathway, type 2). Non-heme Fe-containing MMO's have been isolated from both types of organism, with the type 1 enzymes being the most thoroughly investigated.

Non-heme iron-containing MMO was first isolated from *Methylococcus capsulatus* (type 1). The enzyme consists of three protein components, A–C.[191,192] Component A is believed to contain the site of oxygenase activity; it posseses an $\alpha_2\beta_2\gamma_2$ stoichiometry, with subunit molecular weights of 54, 42, and 17 kDa, respectively, and contains 2.3 mol of iron per mole of protein.[191] Protein B consists of a single subunit of molecular weight 16 kDa.[193] It is devoid of prosthetic groups and believed to serve a regulatory role. The last protein, component C, contains an Fe_2S_2 center and a molecule of FAD; this component is responsible for the interaction with NADH.[194,195] Electrons are believed to flow from NADH to FAD to Fe_2S_2 to component A, independent of the presence of component B.[192,195,196] However, in the absence of component B, monooxygenase activity is lost, and the product of the protein B uncoupled reaction reportedly is water.

MMO from the type II organism *Methylobacterium* SP[197,198] is very similar in composition to the enzyme from type I organisms (Table VII), but apparently lacks the regulatory component (B). Component B is, however, present in MMO from the type II organism *Methylosinus trichosporium*, which is otherwise quite similar in composition to both of the above enzymes (Table VII).[199,200] The *M. trichosporium* enzyme also appears to differ from the type I system in that some oxygenation of substrate occurs in the absence of component B; however, efficient substrate hydroxylation (coupled to NADH oxidation) requires all three components.[200] Thus, reduction of dioxygen to water (a four-electron process) is not observed.

The first attempts to isolate the oxygenase component of MMO were problematic in that an appreciable amount of activity loss accompanied purification.[191,202] Recently, removal of iron from component A of the *M. capsulatus* enzyme followed by reconstitution by incubation with iron was demonstrated to result in at least a 3-fold increase in the specific activity of the protein.[201] This increase in activity was accompanied by an increse in the Fe/protein ratio from 2.3 to 3.3. These results suggest that the iron atoms are the site of oxygenase activity. By using stabilizing agents such as ferrous ion and cysteine, the oxygenase component from *M. trichosporium* has recently been isolated with much greater specific activity.[200] Quantification of iron revealed the presence of four iron ions per protein or two iron ions per $\alpha\beta\gamma$ oligomer. Until recently, little information on the structure, properties, and mode of action of the non-heme iron site was available.

X-ray absorption studies have provided the most detailed information on the structure of the dinuclear iron active site, as crystals of the enzyme have not been reported to date.[203,204] The Fe absorption edge of the oxidized hydroxylase protein from *Methylobacterium* has an edge position typical of ferric iron.[204] The Fourier transform of the EXAFS data displayed two features, assignable to Fe–O/N interactions (four to six O/N at 1.92 Å) and to an Fe···Fe interaction at 3.05 Å, with no evidence for sulfur ligation. X-ray absorption studies on the *M. capsulatus* protein resulted in photoreduction of the dinuclear iron site by the X-ray beam, as evidenced by a ~1.5 eV shift in the edge position to lower energy.[203] The appearance of the $g < 2$ EPR signal (vide infra) in photoreduced samples demonstrated that the mixed-valent, reduced protein was being generated. Fits of the EXAFS data of the photoreduced protein gave 0.8 Fe neighbors at a distance of 3.41 Å and six Fe–O/N interactions at an average distance of ~2.05 Å. Attempts to include contributions from short Fe–oxo interactions were unsuccessful. Comparison of these results with those of similar studies on hemerythrin (section II) and synthetic dinuclear iron complexes (section VII), together with the other spectroscopic data, immediately suggests that the two irons are arranged in a dinuclear site bridged by oxo or hydroxo ligands in the oxidized and mixed-valence forms, respectively. The short $Fe^{3+}\cdots Fe^{3+}$ separation may suggest the presence of a (μ-oxo)bis(μ-carboxylato) core as in hemerythrin or a related multiply bridged center.

Protein A exhibits only a single visible absorption band at ca. 410 nm, which varies in intensity from preparation to preparation[191] (and may result from a zinc–porphyrin-containing impurity).[204] EPR spectra of component A exhibit a signal at $g = 4.3$ that corresponds to <5% of the total iron by double integration and is presumably due to adventitious iron (Figure 19); reduction of the protein with sodium dithionite results in an EPR-detectable species that is only observable below 34 K and gives rise to a rhombic signal with g values less than 2.[204-206] Exposure to excess dithionite results in loss of this signal and the appearance of a new signal at $g = 15$[205] (Figure 19). Comparison of these results with those of similar studies on hemerythrin, RR, and PAP strongly suggest that MMO's contain a dinuclear, oxo- or hydroxo-bridged iron center. Hence, the EPR-silent oxidized form of component A presumably corresponds to an antiferromagnetically coupled Fe(III)–Fe(III) pair. One-electron reduction of the

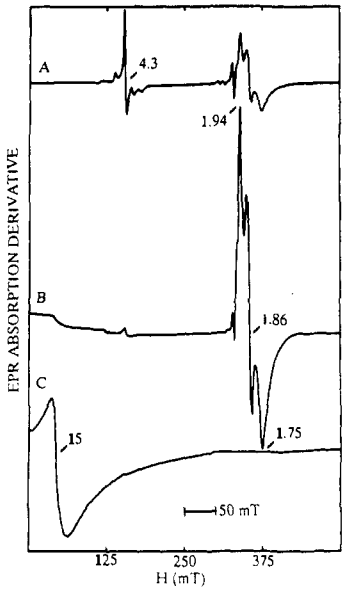

Figure 19. X-Band EPR spectra of the hydroxylase component of MMO from *Methylosinus* in various oxidation levels: (A) oxidized, (B) partially reduced, (C) totally reduced (reprinted from ref 205; copyright 1988 Journal of Biological Chemistry).

dinuclear species by dithionite then generates a less strongly coupled Fe(II)···Fe(III) site, which gives rise to the characteristic $g < 2.00$ EPR signal. Further reduction of the protein produces a weakly coupled Fe(II),Fe(II) species.

These assignments have been verified by Mössbauer spectroscopy.[199,204] The oxidized protein shows a single quadrupole doublet with $\Delta E_Q = 1.07$ mm/s and $\delta = 0.50$ mm/s at 4.2 K; field-dependence studies clearly indicated that the iron center was diamagnetic, containing an even number of Fe^{3+} sites. The Mössbauer spectra of the fully reduced form of this protein contain two quadrupole doublets, with parameters characteristic of Fe^{2+} ($\Delta E_Q = 3.14$, ~2.4 mm/s and $\delta = 1.30$, ~1.3 mm/s at 4.2 K).

VI. Additional and Proposed Oxo-Bridged Dinuclear Iron Proteins

Rubrerythrin is a non-heme iron-containing protein of unknown function from the anaerobic bacterium *Desulfovibrio desulfuricans*. The protein contains four atoms of iron and consists of two identical 21.9-kDa subunits.[207-209] Spectroscopic results indicate that two of the iron atoms exist as monomeric $Fe(SR)_4$ centers, analogous to the $Fe(SR)_4$ sites of rubredoxin. (Each subunit contains four cysteine residues.) Indeed, the electronic (λ_{max} 492, 365, and 280 nm), Mössbauer ($\Delta E_Q = 0.55$ mm/s, $\delta = 0.27$ mm/s), EPR ($g = 4.3$, 9.4) spectra of the oxidized protein are very similar to those of rubredoxin. However, the midpoint potential of these centers (obtained by redox titrations monitored by EPR spectroscopy) was determined to be +230 mV, ~250 mV more positive than that of the rubredoxins. At 4.2 K, Mössbauer spectra revealed the presence of additional features with $\Delta E_Q = 1.47$ mm/s and $\delta = 0.52$ mm/s, indicative of the presence of high-spin ferric ions with O/N ligands. The magnetic field dependence of the quadrupole doublet revealed that the remaining two irons were diamagnetic ($S = 0$); thus, the two ferric ions must be antiferromagnetically coupled, similar to metHr. Treatment with dithionite resulted in the appearance of a new doublet with parameters typical of high-spin ferrous iron ($\Delta E_Q = 3.14$ mm/s, $\delta = 1.30$ mm/s), indicating that reduction of the iron atoms had occurred. In a manner similar to that of the spectra of deoxyHr, the magnetic-field dependence of the signal indicated that the iron atoms were paramagnetic. An EPR signal arising from the semimet form of this diiron center closely resembles the EPR signals of the mixed-valence forms of hemerythrin, the purple acid phosphatases, and methane monooxygenase, with apparent g values of 1.98, 1.76, and 1.57. Resonance Raman studies of rubrerythrin have identified an enhanced band at 515 cm^{-1}, which shifts ~24 cm^{-1} to lower energy in $H_2{}^{18}O$ and is assigned to a bridging or terminal Fe–O stretch.[210] Interestingly, fits of the redox titration curves require interaction potentials between the different types of iron centers.[209] X-ray-quality crystals of the protein have been obtained,[211] suggesting that the three-dimensional structure may be available in the near future.

Ferritin is an iron-storage protein found in plants, animals, and certain bacteria. Mammalian ferritins consist of 24 ~20-kDa subunits, each subunit containing four antiparallel α-helices.[212,213] The subunits are arranged in a rhombic dodecahedron (432 symmetry) forming a hollow sphere. Up to ca. 4500 irons, bridged by oxo and phosphato ligands, may be accommodated inside this protein shell. Recent EXAFS, EPR, and Mössbauer studies[214-216] indicate that oxo- and carboxylato-bridged iron(III) clusters, including dinuclear species, may be formed during the early stages of iron-core formation.

3-Deoxy-D-*arabino*-heptulosonate-7-phosphate synthase (DAHPS) is the first enzyme in the shikimate pathway that is responsible for aromatic amino acid biosynthesis; it catalyzes the condensation of erythrose 4-phosphate and phosphoenolpyruvate. Three isozymes have been identified in *E. coli*, each of which is inhibited by a different aromatic amino acid (i.e. tyrosine, phenylalanine, and tryptophan) in a feedback mechanism. The purified enzymes possess a visible absorbance band at 350 nm. While Co(II) was the first metal reported to activate the *E. coli* enzymes,[217] some isozymes were later claimed to contain one atom of iron.[218] This was supported by a claimed sequence homology between residues 10–18 of the tyrosine-inhibited *E. coli* enzyme and residues 54–62 of hemerythins.[219] This similarity involved only nine residues, however, and in fact this region of the DAHPS sequence is not conserved in the sequences of the other isozymes, with the amino termini showing little or no homology (six identities in the first 41 residues).[220] Very recently evidence has been presented that DAHPS may not be an iron protein at all but rather a copper metalloenzyme.[221]

VII. Synthetic Complexes

While synthetic dinuclear iron complexes with unsupported oxo bridges display electronic and Mössbauer spectra resembling those of hemerythrin, these compounds do not reproduce other spectroscopic properties of the protein.[222] The report of the 2.2-Å resolution X-ray crystal structure of hemerythrin, which conclusively established the presence of the $Fe_2(\mu\text{-}O)(\mu\text{-}O_2CR)_2$ core, sparked efforts to synthesize diiron complexes containing the unique triply bridged core. In 1983, two

TABLE VIII. Comparison of Bond Lengths and Angles for Metazidohemerythrin and Synthetic Iron(III) Complexes

compound[a]	$Fe-O_{oxide}$, Å	Fe···Fe, Å	Fe–O–Fe, deg	ref
metazidohemerythrin	1.64, 1.89	3.25	135	21
$[Fe_2O(O_2CMe)_2(TACN)_2]^{2+}$	1.80, 1.77	3.064	118.3	223
$FeO(O_2CMe)_2((HB(pz)_3)_2$ (2)	1.780, 1.788	3.146	123.6	224, 225
$Fe_2(O_2CMe)_2(TPBN)_2$	1.794	3.129	121.3	226
$[Fe_2O(O_2CPh)L_2]^+$ (8)	1.777, 1.799	3.218	128.3	227
$Fe_2O(O_2CPh)_2(N3)_2$	1.777, 1.802	3.079	118.7	228
$Fe_2O(O_2CMe)_2(bipy)_2Cl_2$ (6)	1.783, 1.787	3.151	123.9	229
$[Fe_2O(O_2CMe)_2(tmip)_2]^{2+}$	1.800	3.158	122.7	230
$Fe_2O(O_2CMe)_2[[OP(OEt)_2]_3Co(C_5H_5)]_2$	1.799, 1.799	3.174	122.4	231

[a] N3 ≡ bis(2-benzimidazolylmethyl)amine, TPBN ≡ tetrakis(2-pyridylmethyl)-1,4-butanediamine, L ≡ N-(*o*-hydroxybenzyl)-*N*,*N*-bis(2-pyridylmethyl)amine, tmip, ≡ tris(N-methylimidazol-2-yl)phosphine.

TABLE IX. Comparison of Physical Properties of Methemerythrins and Synthetic Fe(III) Complexes

	$metN_3Hr$	$[Fe_2O(O_2CMe)_2(TACN)_2]^{2+}$ (1)	$Fe_2O(O_2CMe)_2(HB(pz)_3)_2$ (2)	$Fe_2O(O_2CMe)_2(bipy)_2Cl_2$ (6)	$Fe_2O(O_2CMe)_2(TPBN)_2$	$Fe_2O(O_2CPh)_2(N3)_2$
UV-VIS, nm (ε)	326 (3375)	323 (2979)	339 (4635)	329 (3030)	348 (3678)	355 (4000)
	380 (sh)	374 (sh)	358 (sh)		470 (554)	485 (310, sh)
	446 (1850,br)	448 (339)	457 (505)		505 (493)	525 (110)
	680 (95)	491 (sh)	492 (466)	464 (br,sh)	730 (78.5)	560 (50,sh)
	1010 (5.1)	701 (41)	955 (3.5)			620 (50)
J, cm^{-1}	-134[a]	-115	-121	-132	NR[b]	-117
ν_s(Fe–O–Fe), cm^{-1}	507	540	528	NR	NR	545
ν_{as}(Fe–O–Fe). cm^{-1}	770	749	751	NR	725	745
ref	59, 64, 63	223, 240	224, 225, 238	229	226	228

[a] metHr. [b] NR = not reported.

research groups independently reported the synthesis of such complexes using the tridentate N-based ligands 1,4,7-triazacyclononane (TACN)[223] and hydrotris(1-pyrazolyl)borate ($HB(pz)_3^-$).[224] X-ray diffraction studies of these complexes, $[Fe(III)_2O(O_2CMe)_2(TACN)_2]^{2+}$ (1) and $Fe(III)_2(O_2CMe)_2(HB(pz)_3)_2$ (2), revealed that they are excellent structural models for the diiron core of hemerythrin, accurately reproducing the geometries about the iron centers (Figure 20 and Table VIII). The use of similar ligands based on pyridine, benzimidazole, a phosphite, and imidazole has also produced complexes possessing the $[Fe(III)_2O(O_2CR)_2]^{2+}$ core (Table VIII).[226,228,230,231]

The TACN and $HB(pz)_3^-$ complexes are the best characterized and possess physical characteristics similar to those of metHr (Table IX). Infrared, Raman, and resonance Raman studies[225,232,233] on the ^{16}O- and ^{18}O-containing species have allowed identification of the Fe–O–Fe stretching frequencies. In contrast to those of unsupported oxo-bridged diiron complexes, these vibrations correspond closely to those of metHr (Table IX). As discussed in earlier sections, comparison of the magnetic and Mössbauer spectroscopic properties of the diiron proteins and synthetic oxide-bridged diiron complexes led to the proposal of the existence of analogous diiron units in the proteins. Perhaps the most striking similarity is the magnitude of the antiferromagnetic spin exchange between the metal centers: the coupling constants (J) range from -115 to -132 cm^{-1} for the triply bridged synthetic models versus -134 cm^{-1} for methemerythrin (Table IX). Complexes 1 and 2 have also been used to show that EXAFS is sensitive to the presence of short Fe–μ-oxo interactions[234] and have served as models to establish the existence of such units in Hr, RR, and MMO.

The $HB(pz)_3^-$ complex, 2, can be reversibly protonated to give $[Fe(III)_2(\mu\text{-}OH)(\mu\text{-}O_2CMe)_2(HB(pz)_3)_2]^+$ (3);[235] protonation of the bridging oxo ligand results in an increase in the $Fe-O_{bridge}$ distance of nearly 0.2 Å and

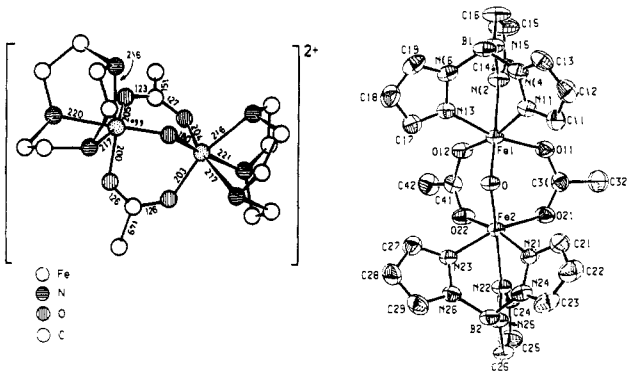

Figure 20. Structures of synthetic oxide-bridged dinuclear iron complexes: (a) $[Fe_2O(O_2CMe)_2(TACN)_2]^{2+}$ (1) (reprinted from ref 223; copyright 1983 VCH), (b) $Fe_2O(O_2CMe)_2(HB(pz)_3)_2$ (2) (reprinted from ref 224; copyright 1983 American Chemical Society).

a corresponding increase in the Fe···Fe separation to 3.439 Å. Although the bridge angle is essentially unchanged, the magnitude of the antiferromagnetic coupling between the iron centers is reduced to -17 cm^{-1}. Protonation of the bridging oxo ligand apparently labilizes the $Fe_2O(O_2CR)_2$ core toward carboxylate substitution. This property has been exploited to synthesize $Fe(III)_2O(O_2P(OPh)_2)_2(HB(pz)_3)_2$ (4), and other analogues in which the acetate ligands of complex 2 have been replaced with diphenyl phosphate and diphenylphosphinate ligands.[236,237] Recently analogues of the TACN complex, 1, have also been prepared where hydrogen phosphate, hydrogen arsenate, chromate, and phenylphosphate replace the bridging acetates (however, only the last two have been structurally characterized).[238] The bridging phosphate groups may be relevant to the chemistry of the purple acid phosphatases.

A model for deoxyhemerythrin has also been prepared with Me_3TACN,[239] $[Fe(II)_2(\mu\text{-}OH)(\mu\text{-}O_2CMe)_2$-

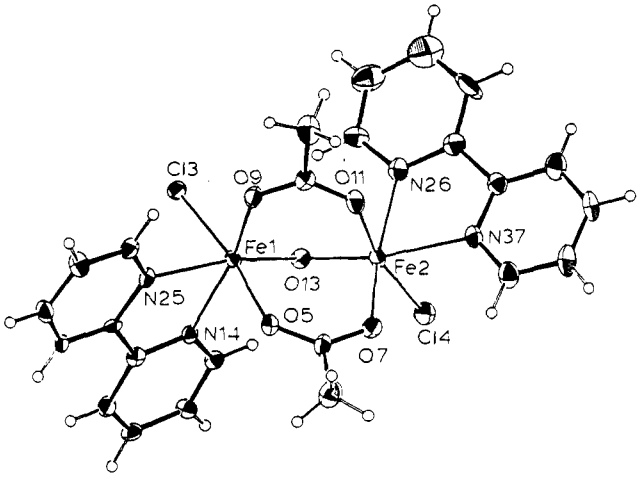

Figure 21. ORTEP drawing of $Fe_2O(O_2CPh)_2(bipy)_2(Cl)_2$ (4) (reprinted from ref 229; copyright 1988 American Chemical Society), with potentially labile coordination sites on each iron atom.

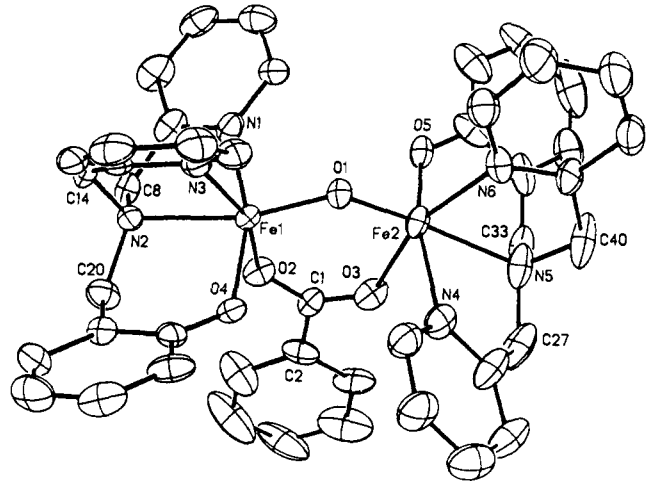

Figure 22. ORTEP drawing of $[Fe_2O(O_2CPh)L_2]^+$ (8) (reprinted from ref 227; copyright 1988 American Chemical Society), illustrating the (μ-oxo)mono(μ-carboxylato)diiron core.

$(Me_3TACN)_2]^+$ (5). As a result of the protonation and reduction of the metal centers compared to those of complex 1, complex 5 exhibits a considerably smaller spin coupling constant, $J = -14$ cm^{-1}, comparable to that of deoxyHr. EPR and Mössbauer studies of the electrochemically generated one-electron-reduction product of complex 1 suggest the species may possess the mixed-valence diiron(II,III) core, corresponding to semimetHr;[240] however, isolation of this species has not proved possible to date.

A number of complexes containing diiron cores bridged by a pair of carboxylates and a phenoxide provided by a polydentate ligand have also been prepared.[241-247] While these reproduce some of the spectroscopic properties of hemerythrin, their relationship to the biological systems is uncertain.

Unfortunately, use of tridentate ligands in the synthesis of the previously described Hr models produces complexes in which all three terminal coordination sites at each metal are blocked, precluding investigation of substrate or substrate-analogue binding. Reaction of complex, 1, for example, with such reagents has been shown to result in disruption of the $[Fe_2O(O_2CR)_2]^{2+}$ core.[248] Recently, the synthesis and characterization of triply bridged dinuclear iron complexes employing the bidentate ligand 2,2'-bipyridine (bipy) has been reported;[229,249] this leaves coordination sites on the metal centers available for binding additional ligands. $Fe_2O(O_2CMe)_2(bipy)_2Cl_2$ (6) and $Fe_2O(O_2CPh)_2(bipy)_2(N_3)_2$ (7) have structures very similar to that of metN_3Hr (Table VIII and Figure 21), with the monodentate terminal ligand cis to the oxide bridge as in the protein. The physical properties of 6 and 7 closely approach those of Hr (Table IX) (as do those of the other models). Synthesis of these complexes has been extended to other bidentate ligands.[250]

Recently a novel oxide-bridged iron compound has been shown to yield a visible spectrum that bears a strong resemblance to that of the purple acid phosphatases.[227] $[Fe(III)_2O(O_2CPh)(L)_2]^+$ (8) (L = *N*-(o-hydroxybenzyl)-*N*,*N*-bis(2-pyridylmethyl)amine) (Figure 22) possesses a (μ-oxo)mono(μ-carboxylato) core, which results in a Fe···Fe separation of 3.218 Å, similar to that in Hr and the model complexes with triply bridged cores. Complex 8 exhibits a broad band in its visible spectrum with a maximum at 522 nm (ϵ/Fe = 3300 M^{-1} cm^{-1}); the intensity of this band indicates that the chromophore in the purple phosphatases may be a single Fe(III)–phenoxide unit. Using tris(2-pyridylmethyl)amine and benzoate, acetate, and diphenyl phosphate as bridging ligands, additional members of this class of $Fe_2O(O_2CR)$ complex have been synthesized.[251,252] Thus, like the triply bridged core found in hemerythrin, the doubly bridged core found in ribonucleotide reductase appears readily accessible synthetically. Unique in these last three complexes, the amine nitrogen of the capping ligand is trans to the oxide bridge on one iron but cis to the oxide on the other iron, introducing asymmetry.

Since an oxo- or hydroxo-bridged dinuclear iron unit may also be present at the active site of methane monoxygenase, studies have recently been directly at using synthetic oxo-bridged non-heme iron complexes for the catalytic hydroxylation of hydrocarbons. The first of these studies revealed that trinuclear "basic iron acetate" could catalyze the epoxidation of olefinic alcohol acetates[253] and, in the presence of dioxygen and zinc powder (as a reducing agent), the hydroxylation of adamantane to a mixture of adamantan-1-ol, -2-ol, and adamantanone.[254] In 1988, the O_2–zinc system was extended with use of complex 2, $Fe_2O(O_2CMe)_2(HB(pz)_3)_2$, as catalyst for oxidation of cyclohexane and adamantane to a mixture of the corresponding alcohols and ketones.[255] The catalytic hydroxylation of simple alcohols (ethane, propane) using non-heme catalysts (synthetic oxide-bridged Mn(III) complexes) was also reported, using *tert*-butyl hydroperoxide as the oxidizing agent;[256] similar reactivity was observed with analogous iron species.[229] The observed reactivity parallels the C–H bond dissociation energies; no reaction was observed with methane.[257] Complex 6 also served as an oxygen-transfer catalyst in the presence of dioxygen and zinc powder; however, reaction of cyclohexane was found to give cyclohexanone as the sole product.[229]

VIII. Conclusion

As the results presented above clearly indicate, the dinuclear iron proteins share two major structural features. First, the spectroscopic data (and X-ray results where available) indicate that all contain oxo- or hy-

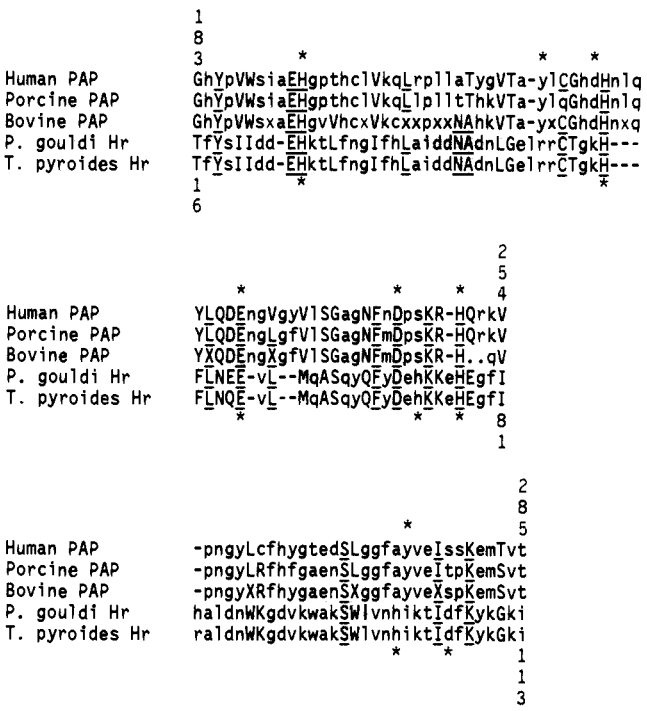

Figure 23. Sequence homology between mammalian purple acid phosphatases and hemerythrins. Conserved residues are indicated by underlined capital letters, and conservative substitutions by capital letters. Asterisks at bottom of lines indicate ligands to iron in hemerythrin (from X-ray structures), while asterisks at top of lines indicate conserved residues that are potential metal ligands in the purple phosphatases (ref 262).

droxo-bridged dinuclear iron units containing in addition one (ribonucleotide reductase) or two (hemerythrin) bridging carboxylate ligands. In the case of the purple phosphatases, the data suggest that both types of structure may occur, with a phosphate- and carboxylate-bridged structure in the oxidized form and a single carboxylate bridge in the reduced form. Both the (μ-oxo)mono(μ-carboxylato) and (μ-oxo)bis(μ-carboxylato)diiron cores are stable fragments that assemble readily from mononuclear species and appropriate ligands, so their presence in a variety of protein environments is not especially surprising (in retrospect, at least). Available data on both proteins and synthetic systems indicate that stepwise reduction of the dinuclear iron center from the diferric to the diferrous oxidation states results in an increased tendency to protonate the bridging oxygen atom and, possibly, to lose one or more bridging ligands altogether, resulting in a dramatic increase in the metal–metal distance. Clearly significant structural flexibility is required on the part of the protein matrix to accommodate such major changes in the dinuclear center.

The second common structural feature pertains to the polypeptide portion of the proteins and suggests a means of providing such a flexible environment. The crystal structures of hemerythrin and ribonucleotide reductase show that, although the two proteins are apparently unrelated in primary structure, both exhibit a tertiary structure comprised of an antiparallel tetra-α-helical bundle. This is a relatively common structural motif in proteins[258] and appears to be substantially stabilized by the opposed α-helix dipole moments as well as by periodic heptad repeats of apolar residues that lead to an interlocking of the helices.[259] Such a structure is apparently well-suited to provide terminal ligands to a dinuclear metal center, with the metal–metal axis either roughly perpendicular (hemerythrin) or parallel (ribonucleotide reductase) to the helix axes. Indeed, such a structure is not unique to iron chemistry, with structurally characterized examples also known for dinuclear copper (hemocyanin)[260] and manganese (Mn catalase),[261] which have the metal–metal axis perpendicular and parallel, respectively, to the helix axis. Consequently, it would not be at all surprising if the remaining dinuclear iron proteins should prove to possess tetra-α-helical structures as well. Although there are no sequence data available for methane monooxygenase and rubrerythrin to explore homologies to either hemerythrin or ribonucleotide reductase, there are parallels between the arrangement of conserved potential metal ligands in the purple phosphatases and hemerythrin, suggesting possible tertiary structure homologies (Figure 23).[262] Also relevant is a recent report that initial binding of iron by apoferritin occurs in the center of the tetra-α-helical bundles,[263] suggesting the possibility of a dinuclear iron intermediate in ferritin core formation.

Despite the core structural similarities and the apparent evidence for convergent protein evolution to stabilize a dinuclear oxo-bridged iron center in these proteins, they exhibit an extraordinarily wide array of functions. Hemerythrin is responsible for reversible dioxygen transport (à la hemoglobin and hemocyanin), while ribonucleotide reductase and methane monooxygenase activate dioxygen for oxidation of a phenol residue and for insertion of an oxygen atom into an unactivated C–H bond, in reactions analogous to the peroxidases (or tyrosinase) and to the cytochromes P450, respectively. In contrast, the purple phosphatases exhibit reversible electron-transfer reactivity that may be physiologically relevant in a control process, as well as using the dinuclear iron center as a Lewis acid in catalysis of phosphate ester hydrolysis via an as yet poorly defined mechanism. This diversity in reactivity is greater than that observed for the better studied heme and iron–sulfur proteins and suggests that the dinuclear oxo-bridged iron center possesses an intrinsic ability to participate in an unprecedented range of chemical and biochemical reactions. It seems likely that additional examples of dinuclear oxo-bridged iron proteins catalyzing these and perhaps other types of reaction remain to be discovered, given their relative insensitivity to detection by simple spectroscopic means.

How then does a particular protein select and control one of these modes of reactivity of a common (μ-oxo)-mono(μ-carboxylato) or (μ-oxo)bis(μ-carboxylato)diiron center? The answer to this question will require detailed structural data on the purple phosphatases and methane monooxygenase, in addition to results from more detailed spectroscopic and mechanistic studies on these fascinating systems.

References

(1) Wilkins, R. G.; Harrington, P. C. *Adv. Inorg. Biochem.* **1983**, *5*, 51–85.
(2) Wilkins, P. C.; Wilkins, R. G. *Coord. Chem. Rev.* **1987**, *79*, 195–214.
(3) Antanaitis, B. C.; Aisen, P. *Adv. Inorg. Biochem.* **1983**, *5*, 111–136.
(4) Doi, K.; Antanaitis, B. C.; Aisen, P. *Struct. Bonding (Berlin)* **1988**, *70*, 1–26.

(5) Sjoberg, B.-M.; Graslund, A. *Adv. Inorg. Biochem.* **1983**, *5*, 87–110.
(6) Que, L., Jr.; Scarrow, R. C. *ACS Symp. Ser.* **1988**, *372*, 152–178.
(7) Lippard, S. J. *Angew. Chem., Int. Ed. Eng.* **1988**, *27*, 344–361.
(8) Sanders-Loehr, J. *Prog. Clin. Biol. Res.* **1988**, *274*, 193–209.
(9) Sanders-Loehr, J. In *Iron Carriers and Iron Proteins*; Loehr, T. M., Ed.; VCH Press: New York, 1989; pp 375–466.
(10) Kurtz, D. M., Jr. *Chem. Rev.* **1990**, *90*, 585–606.
(11) Klotz, I. M.; Kurtz, D. M., Jr. *Acc. Chem. Res.* **1984**, *17*, 16–22.
(12) Richardson, D. E.; Reem, R. C.; Solomon, E. I. *J. Am. Chem. Soc.* **1983**, *105*, 7780–7781.
(13) Babcock, L. M.; Bradic, Z.; Harrington, P. C.; Wilkins, R. G.; Yoneda, G. S. *J. Am. Chem. Soc.* **1980**, *102*, 2849–2850.
(14) Muhoberac, B. B.; Wharton, D. C.; Babcock, L. M.; Harrington, P. C.; Wilkins, R. G. *Biochim. Biophys. Acta* **1980**, *626*, 337–345.
(15) Hendrickson, W. A.; Klippenstein, G. L.; Ward, K. B. *Proc. Natl. Acad. Sci., U.S.A.* **1975**, *72*, 2160–2164.
(16) Stenkamp, R. E.; Sieker, L. C.; Jensen, L. H. *J. Mol. Biol.* **1978**, *126*, 457–466.
(17) Sieker, L. C.; Bolles, L.; Stenkamp, R. E.; Jensen, L. H.; Appleby, C. A. *J. Mol. Biol.* **1981**, *148*, 493–494.
(18) Stenkamp, R. E.; Sieker, L. C.; Jensen, L. H. *Acta Crystallogr.* **1982**, *B38*, 784–792.
(19) Stenkamp, R. E.; Sieker, L. C.; Jensen. L. H. *J. Inorg. Biochem.* **1983**. *19*, 247–253.
(20) Smith, J. L.; Hendrickson, W. A.; Addison, A. W. *Nature* **1983**, *303*, 86–88.
(21) Stenkamp, R. E.; Sieker, L. C.; Jensen, L. H. *Acta Crystallogr.* **1983**, *B39*, 697–703.
(22) Stenkamp, R. E.; Sieker, L. C.; Jensen, L. H. *J. Am. Chem. Soc.* **1984**, *106*, 618–622.
(23) Stenkamp, R. E.; Sieker, L. C.; Jensen, L. H.; McCallum, J. D.; Sanders-Loehr, J. *Proc. Natl. Acad. Sci. U.S.A.* **1985**, *82*, 713–716.
(24) Sheriff, S.; Hendrickson, W. A.; Smith, J. L. *J. Mol. Biol.* **1987**, *197*, 273–296.
(25) Sheriff, S.; Hendrickson, W. A.; Smith, J. L. *Life Chem. Rep. Suppl. Ser.* **1982**, *1*, 305–308.
(26) Stenkamp, R. E.; Sieker, L. C.; Jensen, L. H.; Sanders-Loehr, J. *Nature* **1981**, *291*, 263–264.
(27) Hendrickson, W. A. *Nav. Res. Rev.* **1978**, *31*, 1–20.
(28) Stenkamp, R. E.; Sieker, L. C.; Jensen, L. H. *Proc. Natl. Acad. Sci. U.S.A.* **1976**, *73*, 349–351.
(29) Hendrickson, W. A.; Ward, K. B. *J. Biol. Chem.* **1977**, *252*, 3012–3018.
(30) Darnall, D. W.; Garbett, K.; Klotz, I. M.; Aktipis, S.; Keresztes-Nagy, S. *Arch. Biochem. Biophys.* **1969**, *133*, 103–107.
(31) Klippenstein, G. L.; Van Riper, D. A.; Oosterom, E. A. *J. Biol. Chem.* **1972**, *247*, 5959–5963.
(32) Loehr, J. S.; Lammers, P. J.; Brimhall, B.; Hermodson, M. A. *J. Biol. Chem.* **1978**, *253*, 5726–5731.
(33) Gormley, P. M.; Loehr, J. S.; Brimhall, B.; Hermodson, M. A. *Biochem. Biophys. Res. Commun.* **1978**, *85*, 1360–1366.
(34) Klippenstein, G. L.; Cote, J. L.; Ludlam, S. E. *Biochemistry* **1976**, *15*, 1128–1136.
(35) Klippenstein, G. L.; Holleman, J. W.; Klotz, I. M. *Biochemistry* **1968**, *7*, 3868–3878.
(36) Elam, W. T.; Stern, E. A.; McCallum, J. D.; Sanders-Loehr, J. *J. Am. Chem. Soc.* **1982**, *104*, 6369–6373.
(37) Hendrickson, W. A.; Co, M. S.; Smith, J. L.; Hodgson, K. O.; Klippenstein, G. L. *Proc. Natl. Acad. Sci. U.S.A.* **1982**, *79*, 6255–6259.
(38) Elam, W. T.; Stern, E. A.; McCallum, J. D.; Sanders-Loehr, J. *J. Am. Chem. Soc.* **1983**, *105*, 1919–1923.
(39) Scarrow, R. C.; Maroney, M. J.; Palmer, S. M.; Que, L., Jr.; Roe, A. L.; Salowe, S. P.; Stubbe, J. *J. Am. Chem. Soc.* **1987**, *109*, 7857–7864.
(40) Zhang, K.; Stern, E. A.; Ellis, F.; Sanders-Loehr, J.; Shiemke, A. K. *Biochemistry* **1988**, *27*, 7470–7479.
(41) Okamura, M. Y.; Klotz, I. M.; Johnson, C. E.; Winter, M. R. C.; Williams, R. J. P. *Biochemistry* **1969**, *8*, 1951–1958.
(42) York, J. L.; Bearden, A. J. *Biochemistry* **1970**, *9*, 4549–4554.
(43) Garbett, K.; Johnson, C. E.; Klotz, I. M.; Okamura, M. Y.; Williams, R. J. P. *Arch. Biochem. Biophys.* **1971**, *142*, 574–583.
(44) Clark, P. E.; Webb, J. *Biochemistry* **1981**, *20*, 4628–4632.
(45) Pearce, L. L.; Kurtz, D. M., Jr.; Xia, Y.-M.; Debrunner, P. G. *J. Am. Chem. Soc.* **1987**, *109*, 7286–7293.
(46) Moss, T. H.; Moleski, C.; York, J. L. *Biochemistry* **1971**, *10*, 840–842.
(47) Dawson, J. W.; Gray, H. B.; Hoenig, H. E.; Rossman, G. R.; Schredder, J. M.; Wang, R.-H. *Biochemistry* **1972**, *11*, 461–465.
(48) The convention $H = -2J\vec{S}_1\cdot\vec{S}_2$ is used throughout this article.
(49) York, J. L.; Millett, F. S.; Minor, L. B. *Biochemistry* **1980**, *19*, 2583–2588.
(50) Maroney, M. J.; Lauffer, R. B.; Que, L., Jr.; Kurtz, D. M., Jr. *J. Am. Chem. Soc.* **1984**, *106*, 6445–6446.
(51) Maroney, M. J.; Kurtz, D. M., Jr.; Nocek, J. M.; Pearce, L. L.; Que, L., Jr. *J. Am. Chem. Soc.* **1986**, *108*, 6871–6879.
(52) Dunn, J. B. R.; Shriver, D. F.; Klotz, I. M. *Proc. Natl. Acad. Sci. U.S.A.* **1973**, *70*, 2582–2584.
(53) Dunn, J. B. R.; Shriver, D. F.; Klotz, I. M. *Biochemistry* **1975**, *14*, 2689–2695.
(54) Kurtz, D. M., Jr.; Shriver, D. F.; Klotz, I. M. *J. Am. Chem. Soc.* **1976**, *98*, 5033–5035.
(55) Dunn, J. B. R.; Addison, A. W.; Bruce, R. E.; Loehr, J. S.; Loehr, T. M. *Biochemistry* **1977**, *16*, 1743–1749.
(56) Loehr, T. M.; Shiemke, A. K. *Biol. Appl. Raman Spectrosc.* **1988**, *3*, 439–490.
(57) Vaska, L. *Acc. Chem. Res.* **1976**, *9*, 175–183.
(58) Freier, S. M.; Duff, L. L.; Shriver, D. F.; Klotz, I. M. *Arch. Biochem. Biophys.* **1980**, 4205, 449–463.
(59) Duff, L. L.; Klippenstein, G. L.; Shriver, D. F.; Klotz, I. M. *Proc. Natl. Acad. Sci. U.S.A.* **1981**, *78*, 4138–4140.
(60) McCallum, J. D.; Shiemke, A. K.; Sanders-Loehr, J. *Biochemistry* **1984**, *23*, 2819–2825.
(61) Shiemke, A. K.; Loehr, T. M.; Sanders-Loehr, J. *J. Am. Chem. Soc.* **1986**, *108*, 2437–2443.
(62) Irwin, M. J.; Duff, L. L.; Shriver, D. F.; Klotz, I. M. *Arch. Biochem. Biophys.* **1983**, *224*, 473–478.
(63) Shiemke, A. K.; Loehr, T. M.; Sanders-Loehr, J. *J. Am. Chem. Soc.* **1984**, *106*, 4951–4956.
(64) Garbett, K.; Darnall, D. W.; Klotz, I. M.; Williams, R. J. P. *Arch. Biochem. Biophys.* **1969**, *103*, 419–434.
(65) Gay, R. R.; Solomon, E. I. *J. Am. Chem. Soc.* **1978**, *100*, 1972–1973.
(66) Loehr, J. S.; Loehr, T. M.; Mauk, A. G.; Gray, H. B. *J. Am. Chem. Soc.* **1980**, *102*, 6992–6996.
(67) Harrington, P. C.; deWaal, D. J. A.; Wilkins, R. G. *Arch. Biochem. Biophys.* **1978**, *191*, 444–451.
(68) Guigliarelli, B.; Bertrand, P.; Gayda, J.-P. *J. Chem. Phys.* **1986**, *85*, 1689–1692.
(69) Bertrand, P.; Guigliarelli, B.; Gayda, J. P. *Arch. Biochem. Biophys.* **1986**, *245*, 305–307.
(70) Reem, R. C.; Solomon, E. I. *J. Am. Chem. Soc.* **1984**, *106*, 8323–8325.
(71) Reem, R. C.; Solomon, E. I. *J. Am. Chem. Soc.* **1987**, *109*, 1216–1226.
(72) Freier, S. M.; Duff, L. L.; Van Duyne, R. P.; Klotz, I. M. *Biochemistry* **1979**, *18*, 5372–5376.
(73) Kurtz, D. M., Jr.; Sage, J. T.; Hendrich, M.; Debrunner, P. G.; Lukat, G. S. *J. Biol. Chem.* **1983**, *258*, 2115–2117.
(74) Pearce, L. L.; Utecht, R. E.; Kurtz, D. M., Jr. *Biochemistry* **1987**, *26*, 8709–8717.
(75) McCormick, J. M.; Solomon, E. I. *J. Am. Chem. Soc.* **1990**, *112*, 2005–2007.
(76) Armstrong, F. A.; Harrington, P. C.; Wilkins, R. G. *J. Inorg. Biochem.* **1983**, *18*, 83–91.
(77) Willing, A.; Follman, H.; Auling, G. *Eur. J. Biochem.* **1988**, *170*, 603–611.
(78) Lynch, J. B.; Juarez-Garcia, C.; Münck, E.; Que, L., Jr. *J. Biol. Chem.* **1989**, *264*, 8091–8096.
(79) Joelson, T.; Uhlin, U.; Eklund, H.; Sjoberg, B.-M.; Hahne, S.; Karlsson, M. *J. Biol. Chem.* **1984**, *259*, 9076–9077.
(80) Norlund, P.; Sjoberg, B.-M.; Eklund, H. *Nature*, in press.
(81) Sjoberg, B.-M.; Eklund, H.; Fuchs, J. A.; Carlson, J.; Standart, N. M.; Ruderman, J. V.; Bray, S. J.; Hunt, T. *FEBS Lett.* **1985**, *183*, 99–102.
(82) Bunker, G.; Sjoberg, B.; Reichert, P.; Petersson, L.; Chance, B.; Chance, M. *Fed. Proc.* **1986**, *45*, 1601.
(83) Bunker, G.; Petersson, L.; Sjoberg, B.-M.; Sahlin, M.; Chance, M.; Chance, B.; Ehrenberg, A. *Biochemistry* **1987**, *26*, 4708–4716.
(84) Scarrow, R. C.; Maroney, M. J.; Palmer, S. M.; Que, L., Jr.; Salowe, S. P.; Stubbe, J. *J. Am. Chem. Soc.* **1986**, *108*, 6832–6834.
(85) Atkin, C. L.; Thelander, L.; Reichard, P.; Lang, G. *J. Biol. Chem.* **1973**, *248*, 7464–7472.
(86) Petersson, L.; Graslund, A.; Ehrenberg, A.; Sjoberg, B.-M.; Reichard, P. *J. Biol. Chem.* **1980**, *255*, 6706–6712.
(87) Sahlin, M.; Ehrenberg, A.; Graslund, A.; Sjoberg, B.-M. *J. Biol. Chem.* **1986**, *261*, 2778–2780.
(88) Sahlin, M.; Graslund, A.; Petersson, L.; Ehrenberg, A.; Sjoberg, B.-M. *Biochemistry* **1989**, *28*, 2618–2625.
(89) Larsson, A.; Sjoberg, B.-M. *EMBO J.* **1986**, *5*, 2037–2040.
(90) Sjoberg, B.-M.; Graslund, A.; Loehr, J. S.; Loehr, T. M. *Biochem. Biophys. Res. Commun.* **1980**, *94*, 793–799.
(91) Sjoberg, B.-M.; Loehr, T. M.; Sanders-Loehr, J. *Biochemistry* **1982**, *21*, 96–102.
(92) Sjoberg, B.-M.; Sanders-Loehr, J.; Loehr, T. M. *Biochemistry* **1987**, *26*, 4242–4247.
(93) Backes, G.; Sahlin, M.; Sjoberg, B.-M.; Loehr, T. M.; Sanders-Loehr, J. *Biochemistry* **1989**, *28*, 1923–1929.
(94) Ehrenberg, A.; Reichard, P. *J. Biol. Chem.* **1972**, *247*, 3485–3488.

(95) Sahlin, M.; Petersson, L.; Graslund, A.; Ehrenberg, A.; Sjoberg, B.-M.; Thelander, L. *Biochemistry* **1987**, *26*, 5541–5548.
(96) Barlow, T.; Eliasson, R.; Anton, P.; Reichard, P.; Sjoberg, B.-M. *Proc. Natl. Acad. Sci. U.S.A.* **1983**, *80*, 1492–1495.
(97) Eliasson, R.; Jornvall, H.; Reichard, P. *Proc. Natl. Acad. Sci. U.S.A.* **1986**, *83*, 2373–2377.
(98) Fontecave, M.; Eliasson, R.; Reichard, P. *J. Biol. Chem.* **1987**, *262*, 12325–12331.
(99) Chen, T. T.; Bazer, F. W.; Cetorelli, J. J.; Pollard, W. F.; Roberts, R. M. *J. Biol. Chem.* **1973**, 248, 8560–8566.
(100) Antanaitis, B. C.; Aisen, P. *J. Biol. Chem.* **1984**, *259*, 2066–2069.
(101) Antanaitis, B. C.; Aisen, P.; Lilienthal, H. R. *J. Biol. Chem.* **1983**, 4258, 3166–3172.
(102) Buhi, W. C.; Gray, W. J.; Mansfield, E. A.; Chun, P. W.; Ducsay, C. A.; Bazer, F. W.; Roberts, R. M. *Biochim. Biophys. Acta* **1982**, *701*, 32–38.
(103) Campbell, H. D.; Dionysius, D. A.; Keough, D. T.; Wilson, B. F.; de Jersey, J.; Zerner, B. *Biochem. Biophys. Res. Commun.* **1978**, *82*, 615–620.
(104) Baumbach, G. A.; Ketcham, C. M.; Richardson, D. E.; Bazer, F. W.; Roberts, R. M. *J. Biol. Chem.* **1986**, *261*, 12869–12878.
(105) Sundararajan, T. A.; Sarma. P. S. *Biochem. J.* **1954**, *56*, 125–130.
(106) Singer, M. F.; Fruton, J. S. *J. Biol. Chem.* **1957**, *229*, 111–119.
(107) Campbell, H. D.; Zerner, B. *Biochem. Biophys. Res. Commun.* **1973**, *54*, 1498–1503.
(108) Davis, J. C.; Lin, S. S.; Averill, B. A. *Biochemistry* **1981**, *20*, 4062–4067.
(109) Glomset, J.; Porath, J. *Biochim. Biophys. Acta* **1960**, *39*, 1–8.
(110) Anderson, T. R.; Toverud, S. U. *Arch. Biochem. Biophys.* **1986**, *247*, 131–139.
(111) Hara, A.; Sawada, H.; Kato, T.; Nakayama, T.; Yamamoto, Y.; Matsumoto, Y. *J. Biochemistry* **1984**, *95*, 67–74.
(112) Hayman, A. R.; Warburton, M. J.; Pringle, J. A. S.; Coles, B.; Chambers, T. J. *Biochem. J.* **1989**, *261*, 601–609.
(113) Ketcham, C. M.; Baumbach, G. A.; Bazer, F. W.; Roberts. R. M. *J. Biol. Chem.* **1985**, *260*, 5768–5776.
(114) Uehara, K.; Fugimoto, S.; Taniguchi, T. *J. Biochem.* **1971**, *70*, 183–185.
(115) Uehara, K.; Fujimoto, S.; Taniguchi, T. *J. Biochem.* **1974**, *75*, 627–638.
(116) Fujimoto, S.; Ohara, A.; Uehara, K. *Agric. Biol. Chem.* **1980**, *44*, 1659–1660.
(117) Hefler, S. K.; Averill, B. A. *Biochem. Biophys. Res. Commun.* **1987**, *146*, 1173–1177.
(118) Nochumson, S.; O'Rangers, J. J.; Dimitrov, N. V. *Fed. Proc.* **1974**, *33*, 1378.
(119) Beck, J. L.; McConachie, L. A.; Summors, A. C.; Arnold, W. N.; deJersey, J.; Zerner, B. *Biochim. Biophys. Acta* **1986**, *869*, 61–68.
(120) Fujimoto, S.; Nakagawa, T.; Ishimitsu, S.; Ohara, A. *Chem. Pharm. Bull.* **1977**, *25*, 1459–1462.
(121) Fujimoto, S.; Nakagawa, T.; Ohara, A. *Chem. Pharm. Bull.* **1977**. 425, 3283–3288.
(122) Fujimoto, S.; Nakagawa, T.; Ohara, A. *Agric. Biol. Chem.* **1977**, 441, 599–600.
(123) Igaue, I.; Watabe, H.; Takahashi, K.; Takekashi, M.; Morota, A. *Agric. Biol. Chem.* **1976**, 440, 823–825.
(124) Glew, R. H.; Heath, E. C. *J. Biol. Chem.* **1971**. *246*, 1556–1565.
(125) Jacobs, M. M.; Nyc, J. F.; Brown, D. M. *J. Biol. Chem.* **1971**, *246*, 1419–1425.
(126) Ullah, A. H. J.; Cummins, B. J. *Prep. Biochem.* **1988**, *18*, 37–65.
(127) Buhi, W. C.; Bazer, F. W.; Ducsay, C.; Chun, P. W.; Roberts, R. M. *Fed. Proc.* **1979**, *38*, 733.
(128) Davis, J. C.; Averill, B. A. *Proc. Natl. Acad. Sci. USA* **1982**, *79*, 4623–4627.
(129) Antanaitis, B. C.; Aisen, P. *J. Biol. Chem.* **1982**, *257*, 1855–1859.
(130) Schlosnagle, D. C.; Sander, E. G.; Bazer, F. W.; Roberts, R. M. *J. Biol. Chem.* **1976**, *251*, 4680–4685.
(131) Keough, D. T.; Dionysius, D. A.; de Jersey, J.; Zerner, B. *Biochem. Biophys. Res. Commun.* **1980**, *94*, 600–605.
(132) Hunt, D. F.; Yates, J. R., III; Shabanowitz, J.; Zhu, N.-Z.; Zirino, T.; Averill, B. A.; Daurat-Larroque, S. T.; Shewale, J. G.; Roberts, R. M.; Brew, K. *Biochem. Biophys. Res. Commun.* **1987**, *144*, 1154–1160.
(133) Ketcham, C. M.; Roberts, R. M.; Simen, R. C. M.; Nicke, H. S. *J. Biol. Chem.* **1989**, *264*, 557–563.
(134) Simmen, R. C. M.; Srinivas, V.; Roberts, R. M. *DNA* **1989**, *8*, 543–554.
(135) da Cruz e Silva, O. B.; Cohen, P. T. W. *FEBS Lett.* **1987**, *226*, 176–178.
(136) Vincent, J. B.; Averill, B. A. *FEBS Lett.* **1990**, *263*, 265–268.
(137) Antanaitis, B. C.; Strekas, T.; Aisen, P. *J. Biol. Chem.* **1982**, *257*, 3766–3770.
(138) Schlosnagle, D. C.; Bazer, F. W.; Tsibris, J. C. M.; Roberts, R. M. *J. Biol. Chem.* **1974**, *249*, 7574–7579.
(139) Pyrz, J. W.; Sage, J. T.; Debrunner, P. G.; Que, L., Jr. *J. Biol. Chem.* **1986**, *261*, 11015–11020.
(140) Vincent, J. B.; Averill, B. A., Unpublished results.
(141) Burman, S.; Davis, J. C.; Weber, M. J.; Averill, B. A. *Biochem. Biophys. Res. Commun.* **1986**, *136*, 490–497.
(142) Keough, D. T.; Beck, J. L.; de Jersey, J.; Zerner, B. *Biochem. Biophys. Res. Commun.* **1982**, *108*, 1643–1648.
(143) Soltysik, S.; David, S. S.; Stankovich, M. T.; Que, L., Jr. *Recl. Trav. Chim. Pays-Bas* **1987**, *106*, 252.
(144) Day, E. P.; David, S. S.; Peterson, J.; Dunham, W. R.; Bonvoisin, J. J.; Sands, R. H.; Que, L., Jr. *J. Biol. Chem.* **1988**, *263*, 15561–15567.
(145) Doi, K.; Gupta, R.; Aisen, P. *J. Biol. Chem.* **1987**, *262*, 6982–6985.
(146) Kauzlarich, S. M.; Teo, B. K.; Zirino, T.; Burman, S.; Davis, J. C.; Averill, B. A. *Inorg. Chem.* **1986**, *25*, 2781–2785.
(147) DeBrunner, P. G.; Hendrich, M. P.; de Jersey, J.; Keough, D. T.; Sage, J. T.; Zerner, B. *Biochim. Biophys. Acta* **1983**, *745*, 103–106.
(148) Averill, B. A.; Davis, J. C.; Burman, S.; Zirino, T.; Sanders-Loehr, J.; Loehr, T. M.; Sage, J. T.; Debrunner, P. G. *J. Am. Chem. Soc.* **1987**, *109*, 3760–3767.
(149) Cichutek, K.; Witzel, H.; Parak, F. *Hyperfine Interact.* **1988**, *42*, 885–888.
(150) Lauffer, R. B.; Antanaitis, B. C.; Aisen, P.; Que, L., Jr. *J. Biol. Chem.* **1983**, *258*, 14212–14218.
(151) Sinn, E.; O'Connor, C. J.; de Jersey, J ; Zerner, B. *Inorg. Chim. Acta* **1983**, *78*, L13–L15.
(152) Antanaitis, B. C.; Aisen, P. *J. Biol. Chem.* **1982**, *257*, 5330–5332.
(153) Antanaitis, B. C.; Aisen, P.; Lilienthal, H. R.; Roberts, R. M.; Bazer, F. W. *J. Biol. Chem.* **1980**, *255*, 11204–11209.
(154) Gaber, B. P.; Sheridan, J. P.; Bazer, F. W.; Roberts, R. M. *J. Biol. Chem.* **1979**, *254*, 8340–8342.
(155) Sanders-Loehr, J.; Wheeler, W. D.; Shiemke, A. K.; Averill, B. A.; Loehr, T. M. *J. Am. Chem. Soc.* **1988**, *111*, 8084–8093.
(156) Antanaitis, B. C.; Peisach, J.; Mims, W. B.; Aisen, P. *J. Biol. Chem.* **1985**, *260*, 4572–4574.
(157) Doi, K.; McCracken, J.; Peisach, J. Aisen, P. *J. Biol. Chem.* **1988**, *263*, 5757–5763.
(158) David, S. S.; Que, L., Jr. *J. Inorg. Biochem.* **1989**, *36*, 303.
(159) Antanaitis, B. C.; Aisen, P. *J. Biol. Chem.* **1985**, *260*, 751–756.
(160) Rezyapkin, V. I.; Lenova, L. E.; Komkova, A. I. *Biokhimiya* **1985**, *50*, 1067–1075.
(161) Kawabe, H.; Sugiura, Y.; Terauchi, M.; Tanaka, H. *Biochim. Biophys. Acta* **1984**, *784*, 81–89.
(162) Uehara, K.; Fujimoto, S.; Taniguchi, T.; Nakai, K. *J. Biochem.* **1974**, *75*, 639–649.
(163) Sugiura, Y.; Kawabe, H.; Tanaka, H. *J. Am. Chem. Soc.* **1980**, *102*, 6581–6582.
(164) Sugiura, Y.; Kawabe, H.; Tanaka, H.; Fujimoto, S.; Ohara, A. *J. Biol. Chem.* **1981**, *256*, 10664–10670.
(165) Olivier-Lilley, G. L.; Hefler, S. K.; Averill, B., unpublished results.
(166) Kawabe, H.; Sugiura, Y.; Tanaka, H. *Biochem. Biophys. Res. Commun.* **1981**, *103*, 327–331.
(167) Sugiura, Y.; Kawabe, H.; Tanaka, H.; Fujimoto, S.; Ohara, A. *J. Am. Chem. Soc.* **1981**, *103*, 963–964.
(168) Vincent, J. B.; Christou, G. *Adv. Inorg. Chem.* **1989**, *33*, 197–257.
(169) Beck, J. L.; de Jersey, J.; Zerner, B.; Hendrich, M. P.; DeBrunner, P. G. *J. Am. Chem. Soc.* **1988**, *110*, 3317–3318.
(170) Beck, J. L.; McArthur, M. J.; de Jersey, J.; Zerner, B. *Inorg. Chim. Acta* **1988**, *153*, 39–44.
(171) Beck, J. L.; Keough, D. T.; de Jersey, J.; Zerner, B. *Biochem. Biophys. Acta* **1984**, *791*, 357–363.
(172) Roberts, R. M.; Bazer, F. W. *Biochem. Biophys. Res. Commun.* **1976**, *68*, 450–455.
(173) Sundararajan, T. A.; Sarma, P. S. *Biochem. J.* **1959**, *71*, 537–544.
(174) Glomset, J. A. *Biochim. Biophys. Acta* **1959**, *32*, 349–357.
(175) Revel, H. R.; Racker, E. *Biochim. Biophys. Acta* **1960**, *43*, 465–476.
(176) Robinson, D. B.; Glew, R. H. *Arch. Biochem. Biophys.* **1981**, *210*, 186–199.
(177) Roberts, R. M.; Bazer, F. W. *BioEssays* **1984**, *1*, 8–11.
(178) Buhi, W. C.; Ducsay, C. A.; Bazer, F. W.; Roberts, R. M. *J. Biol. Chem.* **1982**, *257*, 1712–1723.
(179) Doi, K.; Antanaitis, B. C.; Aisen, P. *J. Biol. Chem.* **1986**, *261*, 14936–14938.
(180) Sibille, J.-C.; Doi, K.; Aisen, P. *J. Biol. Chem.* **1987**, *262*, 59–62.
(181) Schindelmeiser, J.; Munstermann, D.; Witzel, H. *Histochemistry* **1987**, *87*, 13–19.
(182) Schindelmeiser, J.; Schewe, P.; Zonka, T.; Mustermann, D. *Histochemistry* **1989**. *92*, 81–85.

(183) Clark, S. A.; Ambrose, W. W.; Anderson, T. R.; Terrell, R. S.; Toverud, S. U. *J. Bone Miner. Res.* **1989**, *4*, 399–405.
(184) Vincent, J. B.; Averill, B. A. *FASEB J.*, in press.
(185) Zaidi, M.; Moonga, B.; Moss, D. W.; MacIntyre, J. *Biochem. Biophys. Res. Commun.* **1989**, *159*, 68–71.
(186) Murray, M. K.; Malathy, P. V.; Bazer, F. W.; Roberts, R. M. *J. Biol. Chem.* **1989**, 4264, 4143–4150.
(187) Baumbach, G. A.; Saunders, P. T. K.; Bazer, F. W.; Roberts, R. M. *Proc. Natl. Acad. Sci. U.S.A.* **1984**, *81*, 2985–2989.
(188) Saunders, P. T. K.; Renegar, R. H.; Raub, T. J.; Baumbach, G. A.; Atkinson, P. H.; Bazer, F. W.; Roberts, R. M. *J. Biol. Chem.* **1985**, *260*, 3658–3665.
(189) Dalton, H. *Adv. Appl. Microbiol.* **1980**, *26*, 71–87.
(190) Tonge, G. M.; Harrison, D. E. F.; Higgins, I. J. *Biochem. J.* **1977**, *161*, 333–344.
(191) Woodland, M. P.; Dalton, H. *J. Biol. Chem.* **1984**, *259*, 53–59.
(192) Prior, S. D.; Dalton, H. *FEMS Microbiol. Lett.* **1985**, *29*, 105–109.
(193) Green, J.; Dalton, H. *J. Biol. Chem.* **1985**, *260*, 15795–15801.
(194) Lund, J.; Dalton, H. *Eur. J. Biochem.* **1985**, *147*, 291–296.
(195) Lund, J.; Woodland, M. P.; Dalton, H. *Eur. J. Biochem.* **1985**, *147*, 297–305.
(196) Green, J.; Dalton, H. *Biochem. J.* **1989**, *259*, 167–172.
(197) Patel, R. N.; Savas, J. C. *J. Bacteriol.* **1987**, *169*, 2313–2317.
(198) Patel, R. N. *Arch. Biochem. Biophys.* **1987**, *252*, 229–236.
(199) Fox, B. G.; Lipscomb, J. D. *Biochem. Biophys. Res. Commun.* **1988**, *154*, 165–170.
(200) Fox, B. G.; Froland, W. A.; Dege, J. E.; Lipscomb, J. D. *J. Biol. Chem.* **1989**, *264*, 10023–10033.
(201) Green, J.; Dalton, H. *J. Biol. Chem.* **1988**, *263*, 17561–17565.
(202) Woodland, M. P.; Dalton, H. *Anal. Biochem.* **1984**, *139*, 459–462.
(203) Ericson, A.; Hedman, B.; Hodgson, K. O.; Green, J.; Dalton, H.; Bentsen, J. G.; Beer, R. H.; Lippard, S. J. *J. Am. Chem. Soc.* **1988**, 4110, 2330–2332.
(204) Prince, R. C.; George, G. N.; Savas, J. C.; Cramer, S. P.; Patel, R. N. *Biochim. Biophys. Acta* **1988**, *952*, 220–229.
(205) Fox, B. G.; Surerus, K. K.; Münck, E.; Lipscomb, J. D. *J. Biol. Chem.* **1988**, *263*, 10553–10556.
(206) Woodland, M. P.; Patil, D. S.; Cammack, R.; Dalton, H. *Biochim. Biophys. Acta* **1986**, *873*, 237–242.
(207) Huynh, B.-H.; Prickril, B. C.; Moura, I.; Moura, J. J. G.; LeGall, J. *R. Trav. Chim. Pasy-Bas* **1987**, *106*, 233.
(208) LeGall, J.; Prickril, B. C.; Moura, I.; Xavier, A. V.; Moura, J. J. G.; Huynh, B.-H. *Biochemistry* **1988**, *27*, 1636–1642.
(209) Moura, I.; Moura, J. J. G.; LeGall, J.; Huynh, B.-H. *J. Inorg. Biochem.* **1989**, 436, 228.
(210) Prickril, B. C.; Kurtz, D. M., Jr.; LeGall, J.; Johnson, M. K.; Huang, H.-Y.; Czernuszewicz, R. *J. Inorg. Biochem.* **1989**, 436, 228.
(211) Sieker, L. C.; Turley, S.; Prickril, B. C.; LeGall, J. *Proteins: Struct., Funct., Genet.* **1988**, *3*, 184–186.
(212) Ford, G. C.; Harrison, P. M.; Rice, D. W.; Smith, J. M. A.; Treffry, A.; White, J. L.; Yariv, J. *Philos. Trans. R. Soc. London* **1984**, *B304*, 561–565.
(213) Thiel, E. C. *Annu. Rev. Biochem.* **1987**, 456, 289–315.
(214) Yang, C.-y.; Meagher, A.; Huynh, B. H.; Sayers, D. E.; Theil, E. C. *Biochemistry* **1987**, 426, 497–503.
(215) Baumiger, E. R.; Harrison, P. M.; Nowik, I.; Treffry, A. *Biochemistry* **1989**, *28*, 5486–5493.
(216) Chasteen, D. N.; Antanaitis, B. C.; Aisen, P. *J. Biol. Chem.* **1985**, *260*, 2926–2929.
(217) Nagano, H.; Zalkin, H. *Arch. Biochem. Biophys.* **1970**, *138*, 58–65.
(218) McCandliss, R. J.; Herrmann, K. M. *Proc. Natl. Acad. Sci. U.S.A.* **1978**, *75*, 4810–4813.
(219) Herrmann, K. M.; Schultz, J.; Hermodson, M. A. *J. Biol. Chem.* **1980**, *255*, 7079–7081.
(220) Ray, J. M.; Yanofsky, C.; Bauerle, R. *J. Bacteriol.* **1988**, *170*, 5500–5506.
(221) Baasov, T.; Knowles, J. R. *J. Bacteriol.* **1989**, *171*, 6155–6160.
(222) Murray, K. S. *Coord. Chem. Rev.* **1974**, *12*, 1–35.
(223) Wieghardt, K.; Pohl, K.; Gebert, W. *Angew. Chem., Int. Ed. Engl.* **1983**, 22, 727.
(224) Armstrong, W. H.; Lippard, S. J. *J. Am. Chem. Soc.* **1983**, *105*, 4837–4838.
(225) Armstrong, W. H.; Spool, A.; Papaefthymiou, G. C.; Frankel, R. B.; Lippard, S. J. *J. Am. Chem. SOc.* **1984**, *106*, 3653–3667.
(226) Toftlund, H.; Murray, K. S.; Zwack, P. R.; Taylor, L. F.; Anderson, O. P. *J. Chem. Soc., Chem. Commun.* **1986**, 191–193.
(227) Yan, S.; Que, L., Jr.; Taylor, L. F.; Anderson, O. P. *J. Am. Chem. Soc.* **1988**, *110*, 5222–5224.
(228) Gomez-Romero, P.; Casan-Pastor, N.; Ben-Hussein, A.; Jameson, G. B. *J. Am. Chem. Soc.* **1988**, *110*, 1988–1990.
(229) Vincent, J. B.; Huffman, J. C.; Christou, G.; Li, Q.; Nanny, M. A.; Hendrickson, D. N.; Fong, R. H.; Fish, R. H. *J. Am. Chem. Soc.* **1988**, *110*, 6898–6900.
(230) Wu, F.-J.; Kurtz, D. M., Jr. *J. Am. Chem. Soc.* **1989**, *111*, 6563–6572.
(231) Feng, X.; Bott, S. G.; Lippard, S. J. *J. Am. Chem. Soc.* **1989**, *111*, 8046–8047.
(232) Spool, A.; Williams, I. D.; Lippard, S. J. *Inorg. Chem.* **1985**, *24*, 2156–2162.
(233) Czernoszewicz, R. S.; Sheats, J. E.; Spiro, T. G. *Inorg. Chem.* **1987**, *26*, 2063–2067.
(234) Hedman, B.; Co, M. S.; Armstrong, W. H.; Hodgson, K. O.; Lippard, S. J. *Inorg. Chem.* **1986**, *25*, 3708–3711.
(235) Armstrong, W. H.; Lippard, S. J. *J. Am. Chem. Soc.* **1984**, *106*, 4632–4633.
(236) Armstrong, W. H.; Lippard, S. J. *J. Am. Chem. Soc.* **1985**, *107*, 3730–3731.
(237) Turoski, P. N.; Armstrong, W. H.; Roth, M. E.; Lippard, S. J. *J. Am. Chem. Soc.* **1990**, *112*, 681–690.
(238) Drueke, S.; Wieghardt, K.; Nuber, B.; Weiss, J.; Fleischhauer, H.-P.; Gehring, S.; Hasse, W. *J. Am. Chem. Soc.* **1989**, 4111, 8622–8631.
(239) Chaudhuri, P.; Wieghardt, K.; Nuber, B.; Weiss, J. *Angew. Chem., Int. Ed. Engl.* **1985**, *24*, 778–779.
(240) Hartman, J. R.; Rardin, R. L.; Chaudhuri, P.; Pohl, K.; Wieghardt, K.; Nuber, B.; Weiss, J.; Papaefthymiou, G. C.; Frankel, R. B.; Lippard, S. J. *J. Am. Chem. Soc.* **1987**, *109*, 7387–7396.
(241) Nishida, Y.; Haga, S.; Tokii, T. *Chem. Lett.* **1989**, 109–112.
(242) Borovik, A. S.; Que, L., Jr. *J. Am. Chem. Soc.* **1988**, 4110, 2345–2347.
(243) Borovik, A. S.; Que, L., Jr.; Papaefthymiou, V.; Münck, E.; Taylor, L. F.; Anderson, O. P. *J. Am. Chem. Soc.* **1988**, 4110, 1986–1988.
(244) Suzuki, M.; Oshio, H.; Uehara, A.; Endo, K.; Yanaga, M.; Kida, S.; Saito, K. *Bull. Chem. Soc. Jpn.* **1988**, *61*, 3907–3913.
(245) Borovik, A. S.; Murch, B. P.; Que, L., Jr.; Papaefthymiou, V.; Münck, E. *J. Am. Chem. Soc.* **1987**, *109*, 7190–7191.
(246) Suzuki, M.; Uehara, A.; Oshio, H.; Endo, K.; Yanaga, M.; Kida, S.; Saito, K. *Bull Chem. Soc. Jpn.* **1987**, *60*, 3547–3555.
(247) Suzuki, M.; Uehara, A.; Endo, K. *Inorg. Chim. Acta* **1986**, *123*, L9–L10.
(248) Wieghardt, K.; Pohl, K.; Ventur, D. *Angew. Chem., Int. Ed. Engl.* **1985**, *24*, 392–393.
(249) Christmas, C.; Vincent, J. B.; Huffman, J. C.; Christou, G., unpublished results.
(250) Beer, R. H.; Tolman, W. B.; Bott, S. G.; Lippard, S. J. *Inorg. Chem.* **1989**, 428, 4559–4561.
(251) Yan, S.; Cox, D. D.; Pearce, L. L.; Juarez-Garcia, C.; Que, L., Jr.; Zhang, J. H.; O'Connor, C. J. *Inorg. Chem.* **1989**, 428, 2507–2509.
(252) Norman, R. E.; Yan, S.; Que, L., Jr.; Backes, G.; Ling, J.; Sanders-Loehr, J.; Zhang, J. H.; O'Connor, C. J. *J. Am. Chem. Soc.* **1990**, *112*, 1554–1562.
(253) Ito, S.; Inone, K.; Mastumoto, M. *J. Am. Chem. SOc.* **1982**, *104*, 6450–6452.
(254) Barton, D. H. R.; Gastiger, M. J.; Motherwell, W. B. *J. Chem. Soc., Chem. Commun.* **1983**, 731–733.
(255) Kitajima, N.; Fukui, H.; Moro-oka, Y. *J. Chem. Soc., Chem. Commun.* **1988**, 485–486.
(256) Fish, R. H.; Fong, R. H.; Vincent, J. B.; Christou, G. *J. Chem. Soc., Chem. Commun.* **1988**, 1504–1506.
(257) Fong, R. H.; Vincent, J. B.; Christou, G.; Fish, R. H., unpublished results.
(258) Presnell, S. R.; Cohen, F. E. *Proc. Natl. Acad. Sci. U.S.A.* **1989**, 486, 6592–6596.
(259) Cohen, C.; Parry, D. A. D. *Proteins: Struct., Funct., Genet.* **1990**, *7*, 1–15.
(260) Volbeda, A.; Hol, W. G. J. *J. Mol. Biol.* **1989**, *206*, 531–546.
(261) Barynin, V. V.; Vagin, A. A.; Melik-Adamyan, V. R.; Grebenko, A. I.; Khangulov, S. V.; Popov, A. N.; Andrianova, M. E.; Vainstafein, A. B. K. *Dokl. Akad. Nauk SSSR* **1986**, *288*, 877–880.
(262) Vincent, J. B.; Averill, B. A., unpublished results.
(263) Lawson, D. M.; Treffry, A.; Artymiuk, P. J.; Harrison, P. M.; Yewdall, S. J.; Luzzago, A.; Cesareni, G.; Levi, S.; Arosio, P. *FEBS Lett.* **1989**, *254*, 207–210.